




Article

Succession of Microbial Community in a Small Water Body within the Alluvial Aquifer of a Large River

Antonija Kulaš¹, Tamara Marković², Petar Žutinić^{1,*}, Katarina Kajan^{3,4}, Igor Karlović², Sandi Orlić^{3,4}, Emre Keskin⁵, Vilim Filipović⁶ and Marija Gligora Udovič¹

¹ Department of Biology, Faculty of Science, University of Zagreb, Rooseveltov trg 6, HR-10000 Zagreb, Croatia; antonija.kulas@biol.pmf.hr (A.K.); marija.gligora.udovic@biol.pmf.hr (M.G.U.)

² Department of Hydrogeology and Engineering Geology, Croatian Geological Survey, Sachsova 2, HR-10000 Zagreb, Croatia; tmarkovic@hgi-cgs.hr (T.M.); ikarlovic@hgi-cgs.hr (I.K.)

³ Ruđer Bošković Institute, Bijenička cesta 54, HR-10000 Zagreb, Croatia; katarina.kajan@irb.hr (K.K.); sandi.orlic@irb.hr (S.O.)

⁴ Center of Excellence for Science and Technology-Integrating Mediterranean Region (STIM), HR-21000 Split, Croatia

⁵ Evolutionary Genetics Laboratory (eGL), Agricultural Faculty, Ankara University, Ankara TR-06135, Turkey; keskin@ankara.edu.tr

⁶ Department of Soil Amelioration, Faculty of Agriculture, University of Zagreb, HR-10000 Zagreb, Croatia; vfilipovic@agr.hr

* Correspondence: petar.zutinic@biol.pmf.hr; Tel.: +385-(0)1-6189-706

Abstract: Nitrogen is one of the essential elements limiting growth in aquatic environments. Being primarily of anthropogenic origin, it exerts negative impacts on freshwater ecosystems. The present study was carried out at the nitrate-vulnerable zone within the alluvial aquifer of the large lowland Drava River. The main aim was to investigate the ecosystem's functionality by characterizing the bacterial and phytoplankton diversity of a small inactive gravel pit by using interdisciplinary approaches. The phytoplankton community was investigated via traditional microscopy analyses and environmental DNA (eDNA) metabarcoding, while the bacterial community was investigated by a molecular approach (eDNA). Variations in the algal and bacterial community structure indicated a strong correlation with nitrogen compounds. Summer samples were characterized by a high abundance of bloom-forming Cyanobacteria. Following the cyanobacterial breakdown in the colder winter period, Bacillariophyceae and Actinobacteriota became dominant groups. Changes in microbial composition indicated a strong correlation between N forms and algal and bacterial communities. According to the nitrogen dynamics in the alluvial aquifer, we emphasize the importance of small water bodies as potential buffer zones to anthropogenic nitrogen pressures and sentinels of the disturbances displayed as algal blooms within larger freshwater systems.

Keywords: nitrogen; alluvial aquifer; large river; small water body; phytoplankton; bacterial community



Citation: Kulaš, A.; Marković, T.; Žutinić, P.; Kajan, K.; Karlović, I.; Orlić, S.; Keskin, E.; Filipović, V.; Gligora Udovič, M. Succession of Microbial Community in a Small Water Body within the Alluvial Aquifer of a Large River. *Water* **2021**, *13*, 115. <https://doi.org/10.3390/w13020115>

Received: 25 November 2020

Accepted: 30 December 2020

Published: 6 January 2021

Publisher's Note: MDPI stays neutral with regard to jurisdictional claims in published maps and institutional affiliations.



Copyright: © 2021 by the authors. Licensee MDPI, Basel, Switzerland. This article is an open access article distributed under the terms and conditions of the Creative Commons Attribution (CC BY) license (<https://creativecommons.org/licenses/by/4.0/>).

1. Introduction

Various aspects of nutrient dynamics in freshwater ecosystems are of paramount importance for understanding how the productivity of surface waters is controlled and provide the opportunity to analyse the current and future impacts of anthropogenic activities on freshwater ecosystems. In such environments, a large part of the primary production may depend on the recycling of nutrients such as nitrogen compounds [1]. Nitrogen is an essential element that often limits growth in aquatic ecosystems, and a key compound in many biochemical processes that are important for life, but can be harmful in high concentrations [2–4]. Nowadays, anthropogenic activities such as fertilizer synthesis and its widespread application on arable areas, as well as the burning of fossil fuels, significantly increase the N fluxes across different environmental compartments [3–5]. Its environmental

effects on aquatic ecosystems include acidification, anthropogenic eutrophication, degradation of water quality, biodiversity loss, and increased greenhouse gas emission [6–8]. Nitrate (NO_3^-) pollution is causing negative impacts on groundwater and surface water resources with its primary anthropogenic origin [9,10]. An elevated concentration of nitrates is associated with diffuse and point sources such as domestic or industrial wastewaters, atmospheric deposition, and animal farming waste. However, most environmental problems related to nitrate are linked to intensive agriculture production [11], as the nitrogen is used to promote crop growth [12,13]. Alluvial groundwater is particularly vulnerable to nitrate leaching from agricultural soils, since agricultural land is characterized by the presence of shallow groundwater and fertile soil suitable for farming [14,15].

The composition of the microbial community depends on environmental conditions that may affect the ecosystem's function [16–19], as they drive the various processes of recycling, dynamics, and assimilation of nitrogen compounds in freshwater habitats [18–20]. The availability of certain N forms in freshwater habitats influences the composition of the phytoplankton community, increases its productivity, and causes harmful algal blooms [6,21,22]. Bloom-forming species encompass a variety of eukaryotic algae but also Cyanobacteria, a prokaryotic algal group closely related to problematic freshwater nuisances. Cyanobacteria are extremely adaptive and competitive organisms with a long evolutionary history, which endowed them with an array of physiological, morphological, and ecological adaptations to survive in a wide variety of environmental conditions [6,23]. Many species of Cyanobacteria are capable of surviving and even thriving in extremely inhospitable conditions, tolerating desiccation, high temperatures, extreme pH, high salinity, and pesticides, thus illustrating their capacity to acclimate in different kinds of habitats [24]. They are the only planktonic group capable of utilizing atmospheric nitrogen via biological N_2 fixation, and, as such, can circumvent N-limited conditions [25,26]. Cyanobacterial genera capable of diazotrophy retain a competitive advantage over other phytoplankton groups. The ability of some Cyanobacteria to form potentially toxic surface blooms has drawn much attention from the general public [21,27,28]. Worldwide, fewer than 30 species that cause a real nuisance. It is still difficult to generalize their ecological requirements, as they can be ubiquitous, specifically preferring eutrophic conditions [29]. Anthropogenic eutrophication is recognized as a global environmental problem in terms of both freshwater biodiversity loss and harmful algal blooms due to the presence of toxins [30,31]. However, the impact of eutrophication may differ in large rivers and lakes, when compared to smaller water bodies, such as streams, ponds, bogs, and small lakes, as well as groundwater [32]. Generally, the small lowland water bodies support naturally high concentrations of nutrients and range from eutrophic to hypertrophic [33,34]. Despite high nutrient conditions, small lowland water bodies collectively support a very diverse and oftentimes unique biodiversity, often richer than the one found in big rivers or lakes [35]. The consequences of eutrophication on the biodiversity of small water bodies are poorly understood and have yet to be fully explored.

One of the systems characterized by high nitrogen inputs in Croatia is the alluvial aquifer of Drava, the second longest river in Croatia. The aquifer has dozens of small lotic and lentic ecosystems, which play a potentially important role as biogeochemical reactors in nitrogen buffering and recycling. The regime and quality of these small water bodies are under heavy anthropogenic pressure, mainly due to agriculture [36]. To investigate the role of these small water bodies the nitrogen recycling in the Drava River alluvial area, we have selected a small inactive gravel pit. By employing interdisciplinary approaches, we aim to characterize the ecosystem's functionality, emphasizing bacterial and phytoplankton diversity and its effects on nitrogen recycling along the hydrological transport pathways.

2. Materials and Methods

2.1. Study Area

The study area, situated in the Drava River valley, upstream of the town of Varaždin (NW Croatia), belongs to the Black sea catchment and covers an area of approximately

200 km² (Figure 1). On the NW side, the alluvial aquifer is adjoined by the Varaždin Lake, an artificial reservoir of the hydroelectric power plant Varaždin, of which the Drava River watercourse constitutes a natural border in the NE direction. The Plitvica Stream flows at the S-SE edge of the study area, while in the middle there are several active and inactive gravel pits. All gravel pits represent exposed groundwater and vulnerable areas where the contamination of groundwater can occur faster from surface contaminants. In some cases, inactive (abandoned) gravel pits are used as waste (industrial or urban) disposal sites and are becoming a threat to groundwater quality [37–39].

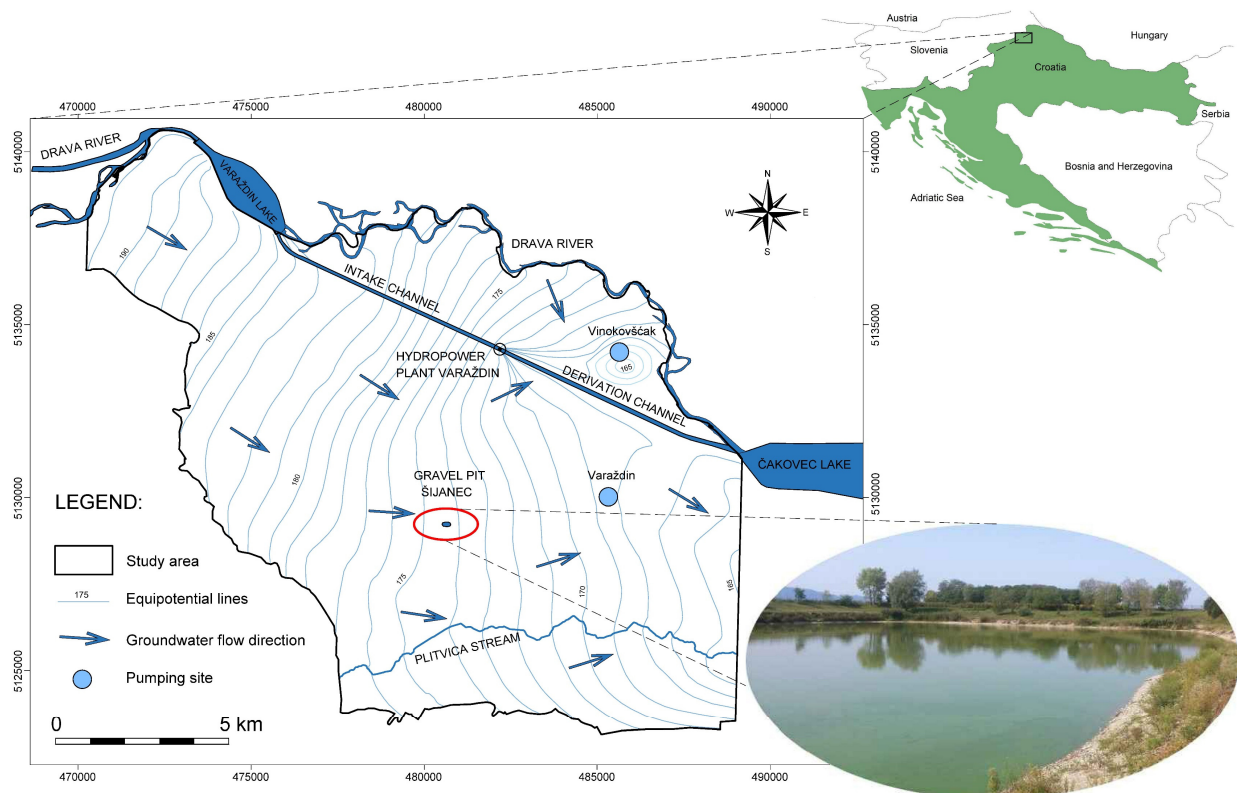


Figure 1. The geographical position of the study area with the location of the sampling area—Šijanec gravel pit—and indication of the groundwater flow direction.

The study area is densely populated, with industrial and intensive agricultural production. The most common type of crops grown are corn, cabbage, potatoes, and vegetables. Extensive poultry farming is present, especially the fattening of chickens, quails, and pheasants, and the breeding of hens [40]. The Varaždin pumping site, one of two in the area, was shut down due to high nitrogen concentrations in groundwater caused by significant anthropogenic activities [41]. Nevertheless, demands for drinking and industrial water rise because of the growing production in the area. The gravel pit in the village of Šijanec was chosen because of its inactivity and accessibility. It is a small pit covering an area of approximately 12,000 m² (Figure 1).

2.2. Sampling and Laboratory Analysis

Phytoplankton and bacterial samples were taken monthly from June 2017 until March 2018 on the deepest point of the gravel pit using the vertical Hydro-Bios water sampler (Hydro-Bios Apparatebau GmbH, Altenholz, Germany). Samples for chemical analysis were taken simultaneously with biological samples and transported in a portable freezer at 4 °C to the laboratory for further analysis. Before sampling, physico-chemical parameters of water, including electrical conductivity (EC), pH, temperature (T), and dissolved oxygen concentration (DO), were measured with a portable WTW Multi 3630 multimeter (Xylem

Analytix, Weilheim, Germany). Water transparency (Z_{SD}) was estimated using a Secchi Disc. Total alkalinity was measured by titration with 1.6 N H_2SO_4 using phenolphthalein and bromocresol green-methyl red as indicators. Dissolved cations (Na^+ , K^+ , Mg^{2+} and Ca^{2+}) and anions (SO_4^{2-} , NO_3^- , Cl^-) were analyzed by ion chromatography using a Dionex ICS-6000 (Thermo Fisher Scientific, Waltham, MA, USA), while NH_4^+ , NO_2^- , and PO_4^{3-} -P were measured spectrophotometrically. Dissolved inorganic and organic carbon (DIC, DOC) and total inorganic and organic carbon (TIC, TOC) were analysed using a HACH QbD1200 TOC analyser (Hach Company, Frederick, MD, USA). The analytical precision of the measurements of cations and anions, indicated by the ionic balance error (IBE), was computed on the basis of ions expressed in $meqL^{-1}$. The IBE value was observed to be within a limit of $<\pm 5\%$ [42,43]. The PHREEQC geochemical code [44] was used to calculate the charge balance and pCO_2 pressure and to study the saturation state of the mineral phases. The samples for Chlorophyll *a* were filtered on Whatman GF/F glass filters (Whatman International Ltd, Kent, UK), extracted in 96% ethanol, and measured for Chl *a* using a UV-VIS spectrophotometer according to compliance monitoring standards [45].

2.3. Microbial Community Analysis

Phytoplankton samples were collected for both morphological and molecular analyses. Samples for morphological analysis were fixed with acid Lugol solution and stored in 250 mL volume glass bottles in the dark at 4 °C. The morphological analysis included a qualitative and quantitative community characterization according to the Utermöhl method [46], using a Zeiss Axiovert 200 inverted microscope (Carl Zeiss, Oberkochen, Germany).

Samples for molecular analysis were collected in sterile plastic bottles and preserved on ice during the transport to the laboratory. In the laboratory, they were immediately filtered on Nucleopore Track-Etch membrane filters (25 mm diameter, 0.4 μm pore size; Whatman International Ltd, Kent, UK) and stored at -20 °C until further processing. DNA was extracted from the frozen filters using DNeasy PowerWaterKit (Qiagen, Hilden, Germany). The manufacturer's instructions were followed with a slight modification in the final step, where 60 μL of sterile DNA-free PCR Grade water was added instead of Qiagen's C6 Solution. The quality of the extracted DNA was assessed with the Shimadzu BioSpec-nano spectrophotometer (Shimadzu Corporation, Kyoto, Japan).

2.4. PCR of the Phytoplankton (Eukaryotic) Community

The hypervariable V9-region of the SSU rRNA gene (ca. 150 base pairs) was amplified from environmental DNA using the universal eukaryotic primer pair [47,48]. The forward and reverse primers were 1391F (5'-GTAC ACACCGCCCGTC-3') and EukB (5'-TGATCCTTCTGCAGGTTACCTAC-3'), designed by Amaral-Zettler and colleagues [49]. Polymerase chain reactions (PCR) contained 1 U of Hot Start Taq DNA Polymerase (New England Biolabs, Ipswich, MA, USA), and for V9 amplification an initial activation step at 95 °C was employed for 5 min, followed by 30 three-step cycles consisting of 94 °C for 30 s, 57 °C for 45 s, and 72 °C for 1 min, followed by a final 2 min extension at 72 °C. PCR products were assessed by visualizing on a 1% agarose gel. Sequencing libraries were constructed using the NEB Next[®] Ultra[™] DNA Library Prep Kit for Illumina (New England Biolabs, Ipswich, MA, USA). Libraries were sequenced on an Illumina MiSeq platform, generating 250-bp paired-end reads (SeqIT GmbH & Co. KG, Kaiserslautern, Germany).

2.5. PCR for the Bacterial Community

The V3-4 region of bacterial rRNA genes was amplified using the forward primer 341 F 5'-CCTACGGGNGGCWGCAG-3' and reverse primer 805 R 5'-GACTACHVGGGTATCTAA TCC-3' [50]. PCR and sequencing were performed in the LGC Genomics GmbH laboratory (Berlin, Germany). The libraries were sequenced on an Illumina MiSeq platform, generating 300-bp paired-end reads.

2.6. Bioinformatic Analysis of the Phytoplankton (Eukaryotic) Community

Sequence reads were analysed using the programs implemented in the OBITools package, as described in De Barba et al. [51]. The quality of the reads was assessed using FastQC. Paired-end reads were aligned using Illumina paired-end, and alignments with quality scores >32 were kept. The aligned data set was demultiplexed using the ngsfilter command, which identified primers and tags and assigned the sequences to each sample. For dereplication, we used the obiuniq command for clustering together strictly identical sequences and keeping the information about their distribution among samples. Sequences shorter than 10 bp, or containing ambiguous nucleotides, or with occurrence lower or equal to 10 were excluded using the obigrep command. The obiclean command was then run to assign the status of “head”, “internal”, or “singleton” to each sequence within a PCR product. All sequences labeled “internal”, corresponding to PCR errors, were discarded. Finally, the taxonomic assignment of OTUs was performed with the ecotag command, combining two reference databases, filtered according to target taxa from NCBI taxonomy and the EMBL database, after running the ecoPCR program [52,53]. Only sequences with a 98% match to the reference sequence were kept. Single-read OTUs were removed from the samples to avoid potential false positives. The final filtered file with taxonomically assigned OTUs of eukaryotic algae groups was used as a basis for all downstream analyses. The DNA sequencing reaction on two samples (September and October 2017) did not yield valid results. A list of commands with related parameters are presented in the Supplementary Materials (S1). Raw demultiplexed reads were deposited at the ENA’s Sequence Read Archive and are publicly available under project number PRJEB40961.

2.7. Bioinformatic Analysis of the Bacterial Community

The quality of the reads was assessed using FastQC. Paired-end reads were quality-trimmed using the bbdduk function and merged using the bbmerge function of the BBMap package 34.48 (Lawrence Berkeley National Lab., Berkeley, CA, USA) [54]. Merged reads were quality-filtered using QIIME v1.8.0 [55]. Reads with exact barcodes and primers, unambiguous nucleotides, and a minimum length of 250 base pairs were retained. A Chimera check was done using UCHIME [56]. Non-chimeric reads were clustered with SWARM v3.0.0 [57] with default settings into Operational Taxonomic Units (OTUs). The bacterial reads were blasted against the SILVA database release 138 (Max Planck Institute for Marine Microbiology and Jacobs University, Bremen, Germany) using blastn (BLAST v2.9.0) [58]. Nontarget OTUs (chloroplasts, mitochondria), as well as singletons and doubletons, were excluded. The resulting OTUs were filtered by the quality of the blast results ($\geq 98\%$ identity). The DNA sequencing reaction on two samples (February and March 2018) did not yield valid results. Raw demultiplexed reads were deposited at the ENA’s Sequence Read Archive and are publicly available under project number PRJEB40962.

2.8. Statistical Analysis

Statistical analyses were conducted in R v. 4.0.2 [59] using the program packages “vegan”, “fossil”, “factoextra”, “devtools”, and “ggbiplot”, as well as “ggplot2” for all graphical representations. To access the comparability of morphological and molecular methodologies in the phytoplankton community, the taxa lists derived from both approaches were compared with regard to the presence or absence of taxa and community composition. The bacterial community composition was analysed by using the molecular approach. The results for downstream analysis were combined into a single data set for each approach and for each community. The molecular results were transformed into relative abundances to normalize the OTU database [60]. Biomass data obtained by microscopy for the phytoplankton community were transformed following the logarithmic scale [61].

The Shannon, Simpson, and richness indices were calculated for both approaches and both communities as measures of alpha diversity using program packages “Vegan v. 2.5.6” [62].

To test the statistical significance of the environmental parameters and which parameter was singled out depending on the month studied, a principal component analysis (PCA) was performed using the R package “vegan” [62].

Canonical correspondence analyses (CCA) were performed on phytoplankton morphological data and bacterial molecular data to estimate variance in environmental variables for both communities. ANOVA test was applied to test the statistical significance of all axes, and forward selections were used to evaluate the importance of each variable. The logarithm function was used to transform environmental parameters and both community datasets for statistical analysis.

3. Results

3.1. Analysis of Environmental Parameters

The environmental variables of the investigated gravel pit are indicated in Table 1. The highest value of nitrates (NO_3^-) concentration was measured in March (38.4 mg L^{-1}) and the lowest in June (0.62 mg L^{-1}), whereas the maximum concentrations of ammonium (NH_4^+) and nitrites (NO_2^-) were recorded in July (2.75 mg L^{-1} and 0.17 mg L^{-1} , respectively). The highest value of pH was detected in August (9.48), indicating that the water was alkaline. The highest temperature (T) value was recorded in June ($24.2 \text{ }^\circ\text{C}$) and the lowest in February ($1.2 \text{ }^\circ\text{C}$), respectively. The maximum value of dissolved oxygen was measured in August (17.1 mg L^{-1}), and the minimum value was in July (7.1 mg L^{-1}). For electrical conductivity (EC) and bicarbonates (HCO_3^-), the maximum values were recorded in March ($497 \text{ } \mu\text{S cm}^{-1}$ and 249 mg L^{-1} , respectively) and the minimum ones in October ($252 \text{ } \mu\text{S cm}^{-1}$ and 107 mg L^{-1} , respectively). Silicon dioxide (SiO_2) concentrations were high during the warmer period, and the maximum was in September (26.8 mg L^{-1}). During the colder period the concentrations were much lower, and the minimum was in December (7.2 mg L^{-1}). In addition, a change was also observed in the concentrations of calcium, bicarbonates, and $\log p\text{CO}_2$ pressure (Table 1), with the lowest concentrations detected in the summer period and the highest concentrations during winter.

Table 1. Ranges of environmental variables in the Šijanec gravel pit during the investigated period.

Variable	Min	Max	Mean	Med	SD
T ($^\circ\text{C}$)	1.2	24.2	13.0	11.5	9.1
EC ($\mu\text{S cm}^{-1}$)	252	497	347	316	99
pH	7.83	9.48	8.49	8.23	0.60
DO (mg L^{-1})	7.1	17.1	12.5	12.7	2.9
$\log p\text{CO}_2$	-4.69	-2.54	-3.44	-3.15	0.74
HCO_3^- (mg L^{-1})	107	249	159	138	54
$\text{PO}_4^{3-}\text{-P}$ (mg L^{-1})	0.01	0.32	0.10	0.05	0.11
TN (mg L^{-1})	0.28	10.15	4.57	4.45	3.54
NH_4^+ (mg L^{-1})	0.01	2.75	0.42	0.09	0.84
NO_2^- (mg L^{-1})	0.05	0.17	0.08	0.07	0.04
NO_3^- (mg L^{-1})	0.6	38.4	15.3	11.1	14.0
TIC (mg L^{-1})	18.44	29.36	23.76	23.06	4.62
DIC (mg L^{-1})	14.50	27.68	21.61	20.19	4.33
TOC (mg L^{-1})	7.20	24.66	16.61	16.25	6.68
DOC (mg L^{-1})	6.13	20.22	14.08	13.82	5.57
Ca^{2+} (mg L^{-1})	20.0	66.1	38.2	31.7	18.3
Mg^{2+} (mg L^{-1})	15.2	20.0	17.4	16.7	1.7
Na^+ (mg L^{-1})	6.9	17.4	12.2	13.3	3.7
K^+ (mg L^{-1})	0.9	1.6	1.1	1.1	0.2
Cl^- (mg L^{-1})	11.8	24.7	17.5	17.3	4.2
SO_4^{2-} (mg L^{-1})	16.0	33.1	24.3	24.8	5.6
SiO_2 (mg L^{-1})	7.2	26.8	15.6	13.0	6.2
Z _{SD} (m)	0.125	0.5	0.28	0.25	0.111
SI _{Calcite}	-0.2	1.1	0.5	0.5	0.4

PCA Analysis

The principal component analysis (PCA) performed for the 24 environmental variables explained 71.1% of the total variance on the first two PC axes. The overall strength of correlations between the samples and environmental parameters are summarized in Table 2. The most important variables for the PC1 axis were TIC, Ca²⁺, and EC (intra-set correlations: 0.271, 0.269, and 0.268, respectively). Regarding the PC2 axis, NH₄⁺ and DO (intra-set correlations: −0.355 and 0.407, respectively) were the variables that weighted most for the ordination. PCA arranged the samples into three groups (Figure 2): the first group consisted of samples from a warmer period of investigation (June, August, September, and October), the second group included a sample from July, while the third one comprised all samples from the colder period of investigation (November, December, January, February, and March).

Table 2. Summary statistics for the first two axes of PCA performed on the environmental variables during the investigated period.

PCA Axis	PC1	PC2
Standard deviation	3.531	2.145
Proportion of variance (%)	51.9	19.2
Cumulative proportion (%)	51.9	71.1
Eigenvalues		
T	−0.246	−0.094
EC	0.268	−0.012
pH	−0.254	0.173
DO	0.030	0.407
logpCO ₂	0.256	−0.184
HCO ₃ [−]	0.237	−0.045
PO ₄ ^{3−} -P	−0.008	−0.126
TN	0.265	−0.021
NH ₄ ⁺	−0.089	−0.355
NO ₂ [−]	−0.154	−0.294
NO ₃ [−]	0.266	0.059
TIC	0.271	−0.067
DIC	0.193	−0.054
TOC	−0.260	−0.028
DOC	−0.249	−0.106
Ca ²⁺	0.269	−0.0003
Mg ²⁺	−0.205	−0.103
Na ⁺	−0.006	0.377
K ⁺	−0.182	−0.263
Cl [−]	0.041	0.368
SO ₄ ^{2−}	−0.156	0.285
SiO ₂	−0.208	0.200
Z _{SD} (Secchi)	−0.079	−0.103
SI _{Calcite}	−0.205	0.127

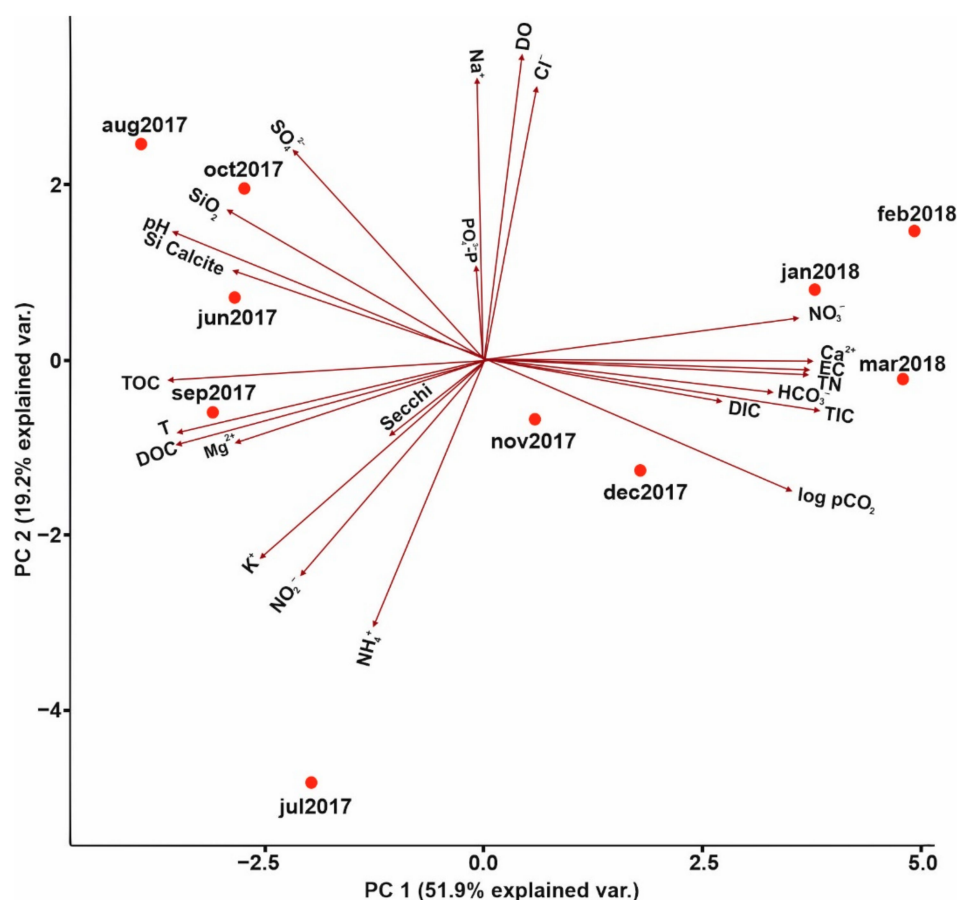


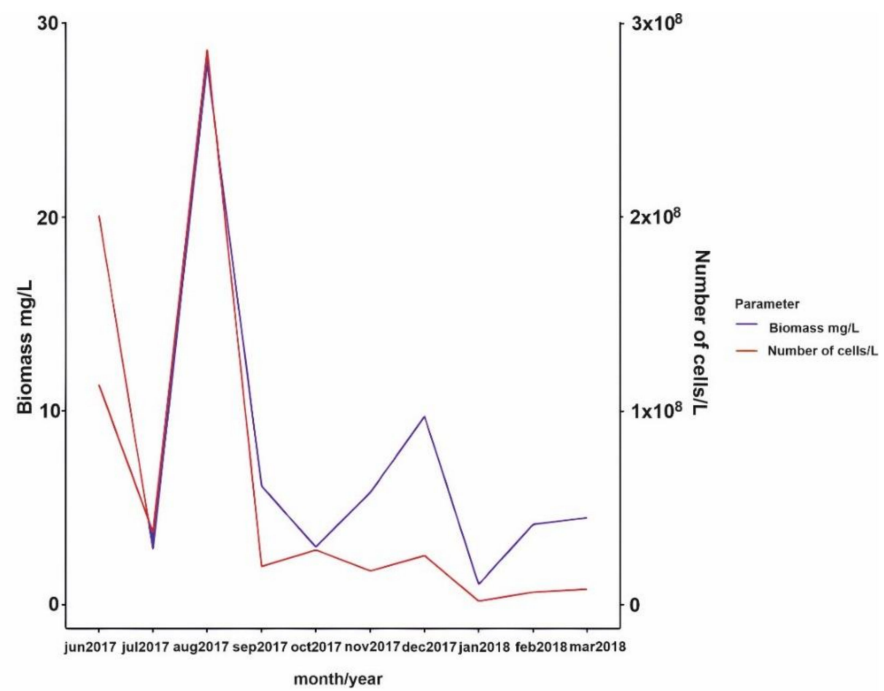
Figure 2. Principal Component Analysis (PCA) ordination of the environmental variables during the investigated period.

3.2. Phytoplankton Succession

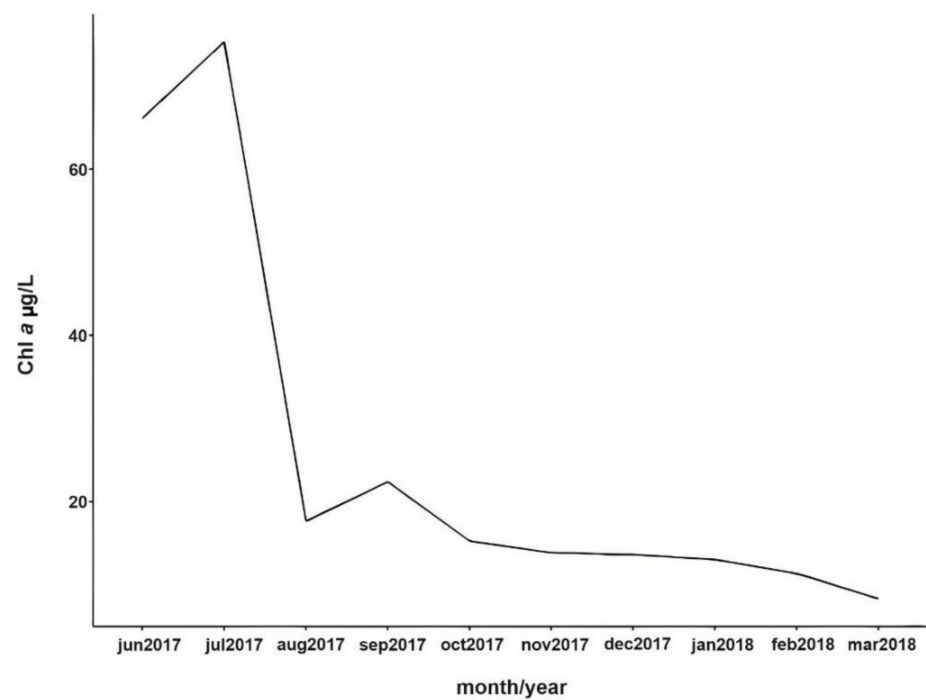
A total of 38 phytoplankton species were recorded by a morphological approach within the 10 samples collected during the investigated period. A total of 47,130 reads clustered into 88 OTUs were detected in the remaining eight samples. OTUs were taxonomically assigned into 30 eukaryotic algal taxa.

Phytoplankton abundance ranged between 1.9×10^6 cells L^{-1} in January 2018 to 2.8×10^8 cells L^{-1} in August 2017. Phytoplankton biomass ranged from 1.05 mg L^{-1} in January 2018 to 27.85 mg L^{-1} in August 2017, related to the cyanobacterial bloom of *Microcystis* spp. (Figure 3a). The chlorophyll *a* value fluctuated from 8.37 μg L^{-1} (March 2018) to 75.3 μg L^{-1} (July 2017). Concurrently, the highest peak of chlorophyll *a* concentration was not recorded during the cyanobacterial bloom in August 2017, but instead in July 2017, during the proliferation of green algae, predominantly *Scenedesmus quadricauda* (Turpin) Brébisson (Figure 3b).

As inferred from the morphological approach, the alpha diversity in the richness, Shannon, and Simpson indices of phytoplankton varied considerably during the investigated period. The maximum value of species richness was recorded in June 2017, while the minimum was noted in February 2018. The Shannon index values ranged from the maximum in October 2017 to the minimum in March 2018. The maximum value of the Simpson index was also noted in October 2017, but the minimum was recorded in June 2017 (Figure 4a). The richness, Shannon, and Simpson indices inferred from the molecular approach did not show the same pattern. The highest value of richness index was recorded in January 2018, while the lowest richness was noted in August 2017. The minimum and maximum values of the Shannon and Simpson indices were reported in July 2017 and June 2017, respectively (Figure 4b).

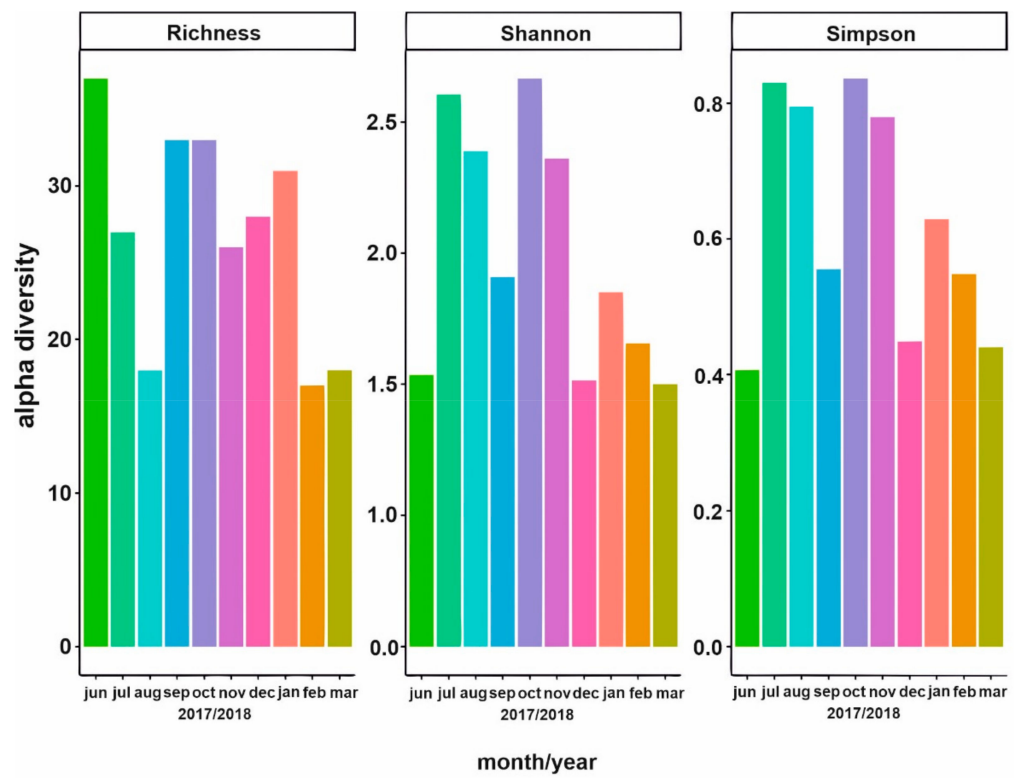


(a)

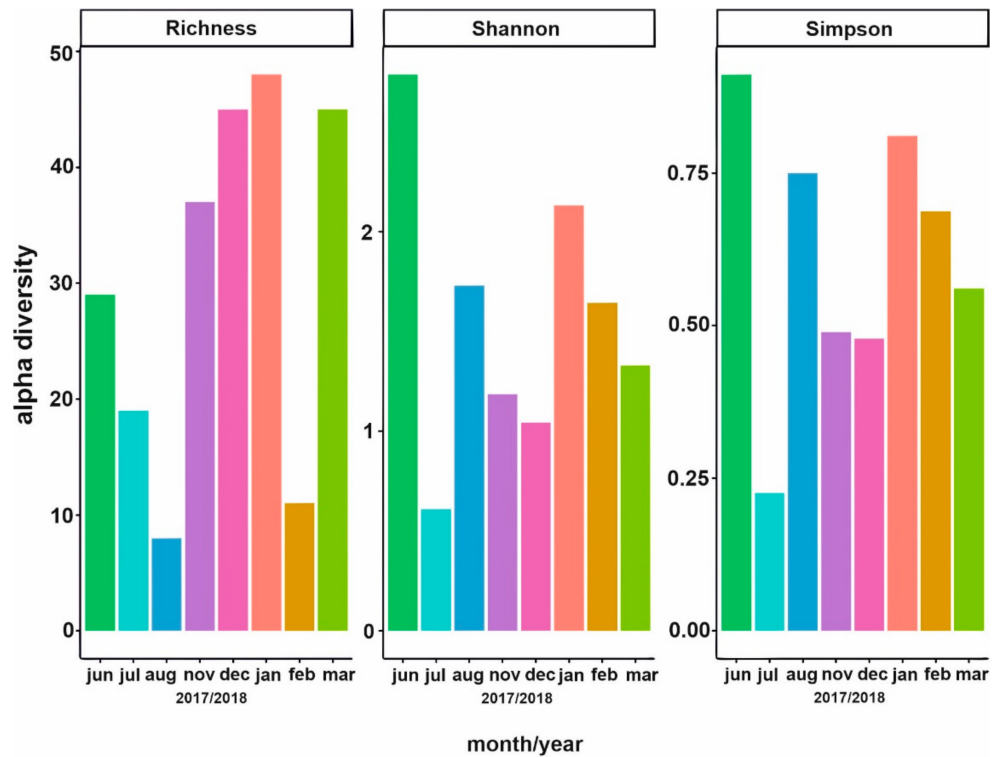


(b)

Figure 3. Phytoplankton: (a) total biomass and abundance; (b) chlorophyll *a* concentration during the investigated period.



(a)



(b)

Figure 4. Alpha diversity of the richness, Shannon, and Simpson indices of the phytoplankton community inferred from the morphological and molecular approach during the investigated period ((a) = morphological approach, (b) = molecular approach).

According to the frequency and biomass, the most dominant species were: filamentous cyanobacterium *Limnothrix redekei* (Goor) Meffert, colonial clathrate cyanobacteria *Microcystis aeruginosa* (Kützing) Kützing and *M. wesenbergii* (Komárek) Komárek ex Komárek, centric diatom *Aulacoseira muzzanensis* (F.Meister) Krammer, pennate diatoms *Ulnaria ulna* (Nitzsch) Compère and *Ulnaria* sp. (Kützing) Compère, cryptophyte *Cryptomonas* sp. Ehrenberg, dinoflagellate *Peridinium* sp. Ehrenberg, and colonial chlorophyte *Scenedesmus quadricauda* (Turpin) Brébisson.

A CCA was performed for the phytoplankton samples, and nine constrained environmental variables (Figure 5) indicated eigenvalues for the first two axes of 0.4328 and 0.3210, respectively, explaining 38.5% of the total variance on the first two axes. A Pearson environment-species permutation for the two significant axes indicated a significant correlation between abiotic constrained values and phytoplankton functional variables. According to the ANOVA permutation test, the ordination of both axes for environmental variables was statistically significant ($p < 0.05$). Canonical coefficients and intra-set correlations on the phytoplankton samples showed that NO_3^- and EC were the most important variables for the ordination axis 1 (intra-set correlation coefficients: 0.6332 and 0.5467, respectively). Regarding axis 2, NO_2^- and NH_4^+ (intra-set correlations -0.8155 and -0.6837 , respectively) were the variables that weighted most for the ordination. At the positive end of both axes, phytoplankton samples were associated with EC, DO, HCO_3^- , and NO_3^- . At the negative end of both axes, phytoplankton samples were associated with pH, T, SiO_2 , NH_4^+ , and NO_2^- . Considering the environmental pressure to phytoplankton, the CCA analysis showed the separation of samples into three groups (Figure 5). The first group, comprised of summer and autumn samples (July to October 2017), correlated with high concentrations of NH_4^+ (2.75 mg L^{-1}), NO_2^- (0.173 mg L^{-1}), and SiO_2 (26.8 mg L^{-1}) and high values of pH (9.48) and T ($24 \text{ }^\circ\text{C}$). The most common species of the group were cyanobacteria *M. aeruginosa* and *M. wesenbergii*, green alga *Scenedesmus quadricauda* and cryptophyte *Cryptomonas* sp. According to the morphological approach, the samples collected in July were characterized by the highest Chl *a* concentration, the dominance of *S. quadricauda*, and the highest concentration of NH_4^+ (2.75 mg L^{-1}). A pronounced increase in the total phytoplankton biomass was recorded in August as a result of *Microcystis* spp. bloom. *M. aeruginosa* and *Cryptomonas* sp. were the descriptive species of the phytoplankton community in September and October, with the continuing decrease of the phytoplankton biomass. The molecular approach did not confirm the same composition, but rather detected the cyanobacterial predominance and a higher contribution of OTUs taxonomically assigned to the *Cryptomonas* genera. According to the morphological approach, the second group, consisting of an outlying sample from June 2017, was characterized by the predominance of filamentous cyanobacterium *Limnothrix redekei* (Goor) Meffert and centric diatom *Aulacoseira muzzanensis* (Meister) Krammer. The molecular approach confirmed the dominance of OTUs taxonomically assigned to the *Aulacoseira* genera as well, but also detected a high number of reads of OTUs taxonomically assigned to genus *Parvodinium*. The third group, composed of winter samples (November 2017 to March 2018), correlated with low T and higher concentrations of NO_3^- (38.4 mg L^{-1}) and HCO_3^- (249 mg L^{-1}) and with mostly constant values of DO (11.9 to 14.7 mg L^{-1}) and EC ($497 \text{ } \mu\text{S cm}^{-1}$). As confirmed by both morphological and molecular approaches, the most dominant species/taxonomically assigned OTUs during the colder period were pennate diatoms (Fragilariaceae) of the genus *Ulnaria*. Dinoflagellate *Peridinium* sp. was recorded only by the morphological approach as the subdominant species in November and January. The higher contribution of the genus *Dinobryon* was confirmed by both analyses during February and March.

As confirmed by both the morphological and molecular approaches, the most dominant species during the colder period were pennate diatoms (Fragilariaceae) of the genus *Ulnaria* with dinoflagellate *Peridinium* sp. as the subdominant species.

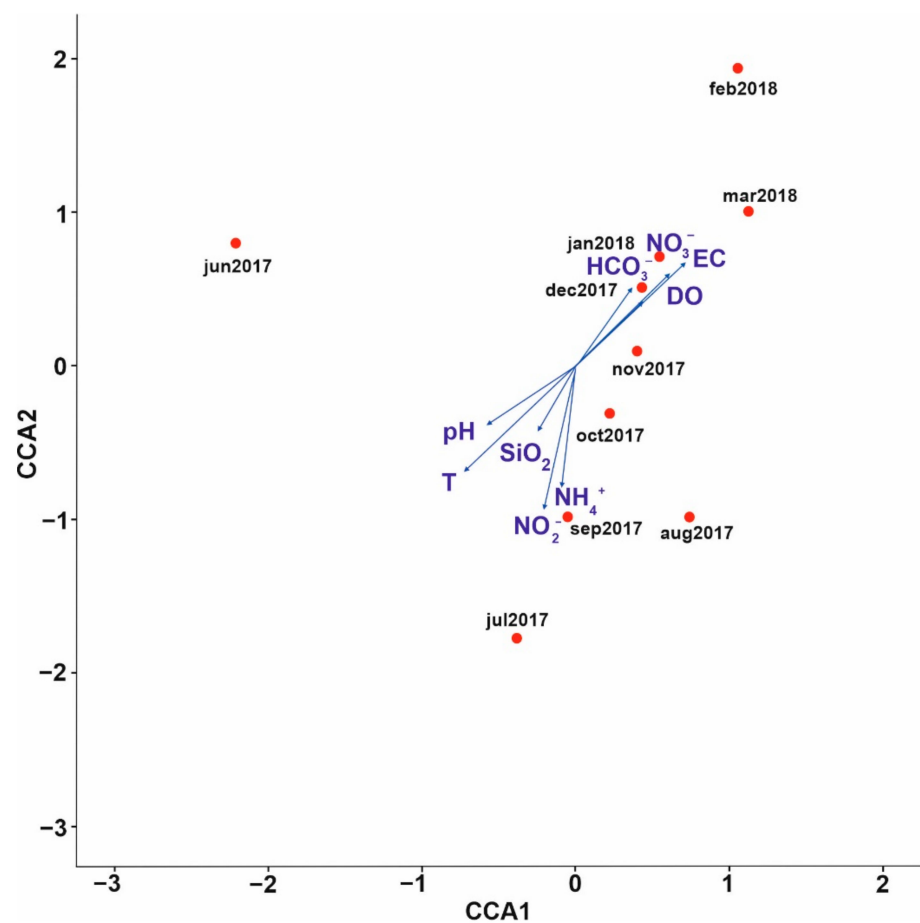


Figure 5. Ordination diagram of the canonical correspondence analysis (CCA) of the phytoplankton community inferred from the morphological approach in correlation to environmental variables during the investigated period.

3.3. Bacterial Community Composition

For the eight samples, a total of 582,900 reads clustered into 1743 OTUs were recorded. Sequence reads were taxonomically assigned into 52 bacterial phyla. The bacterial composition showed a succession of differences between months. The variations of alpha diversity in the rarefied richness, Shannon, and Simpson indices are shown in Figure 6. The highest bacterial richness was recorded in July 2017, and the lowest in October 2017. The Shannon and Simpson indices showed similar results, with the highest values in January 2018 and the lowest in August 2017. Comparing the composition of bacteria and eukaryotic algae inferred from the molecular approach, low values in richness and both indices during the summer period were noted.

According to the percentage of classified OTUs, dominant bacterial phyla were Planctomycetota (22%), Cyanobacteria (64%), Bacteroidota (11%), Actinobacteriota (45%), and Proteobacteria (56%).

The CCA analysis performed on the bacterial community and seven constrained environmental variables (Figure 7) indicated eigenvalues for the first two axes of 0.7131 and 0.6563, respectively, explaining 47.2% of the total variance on the first two axes. A Pearson environment-bacterial community permutation for the two significant axes indicated a significant correlation between abiotic constrained values and bacterial functional variables. According to the ANOVA permutation test, the ordination of both axes for environmental variables was statistically significant ($p < 0.05$). Canonical coefficients and intra-set correlations carried out on the bacterial community samples showed that pH and DO were the most important variables for the ordination axis 1 (intra-set correlation coefficients:

0.6140 and 0.3770, respectively). Regarding axis 2, NO_2^- and NH_4^+ (intra-set correlations: 0.9229 and 0.8706, respectively) were the variables that weighted most for ordination. At the positive end of both axes, the bacterial community's samples were associated with T, pH, and NO_2^- . At the negative end of both axes, the bacterial community's samples were associated with EC and HCO_3^- . Based on the position of the samples related to the CCA1 axis, the bacterial community separated into two groups (Figure 7). The first group, comprised of summer samples (June to September 2017), correlated with a high concentration of NH_4^+ and NO_2^- , and high values of pH and T. According to the percentage of classified OTUs, the most common phyla in the first group were Cyanobacteria, with the most dominant families being Pseudanabaenaceae (June 2017), Microcystaceae (July 2017), and Synechococcaceae and Microcystaceae (August 2017). This was also confirmed by a morphological approach, except for the picocyanobacterium of the genus *Cyanobium*, which is hard to detect under light microscopy. In June, Planctomycetota were codominant with Cyanobacteria. The sample from July was singled out as a result of the codominance of Cyanobacteria and Bacteroidota, which correlated with the concentration of NH_4^+ . The second group, comprising samples from the colder months (October 2017 to January 2018), correlated with low T and higher concentrations of HCO_3^- , DO, and EC. Actinobacteriota was the dominant phylum in October 2017 and January 2018, whilst samples from November and December were dominated by Proteobacteria.

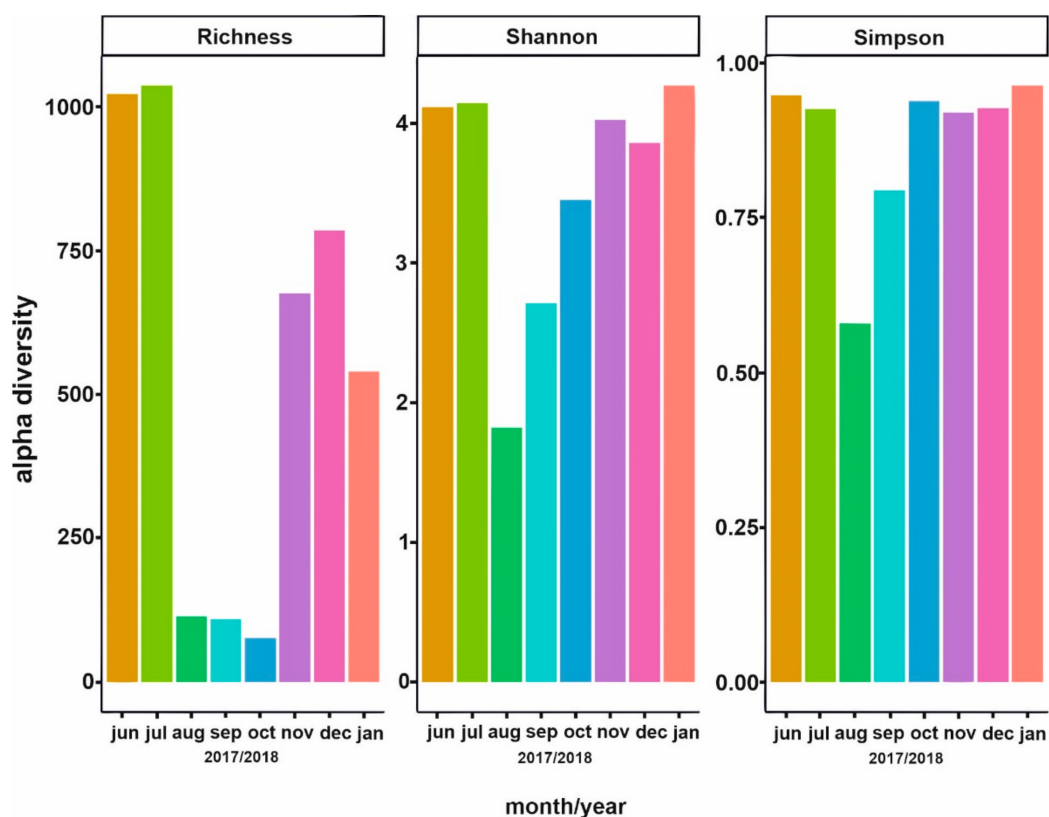


Figure 6. Alpha diversity of the richness, Shannon, and Simpson indices of the bacterial community inferred from the molecular approach during the investigated period.

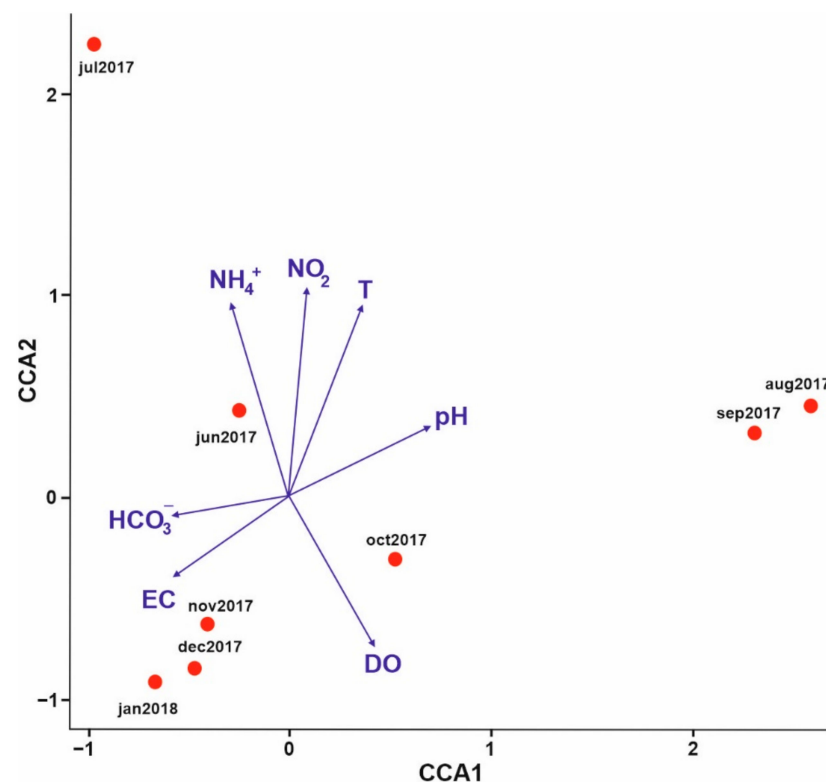


Figure 7. Ordination diagram of the canonical correspondence analysis (CCA) of the bacterial community inferred from the molecular approach in correlation with environmental variables during the investigated period.

4. Discussion

Data on ecology and the importance of small water bodies in alluvial lowlands are still quite scarce, as those systems are not included in the national strategies for the protection of water resources. Within larger freshwater systems, small water bodies act as biochemical reactors because of their potential for supporting high metabolic rates that are often paired with naturally high concentrations of nutrients and trophic conditions [33,34,63]. Their role is modulating nutrient retention and recycling along the hydrological pathways [63]. Even though usually related to eutrophic or hypertrophic conditions, small standing water bodies collectively support a very diverse biodiversity, often with species-richer communities more adapted to eutrophication conditions and to a broad range of physical and chemical conditions than the communities in larger water bodies [38,64]. Eutrophication has been described as a major stressor for the freshwater biodiversity of both large and small water bodies [65,66]. Rosset et al. [32] suggested that the eutrophication management of lowland small water bodies should be regulated differently than for larger freshwater systems, with the conservation efforts focused on the protection of small water bodies representing a mosaic of trophic conditions (and acting as hosts of regional biodiversity).

Seasonal changes with complex dynamic phases govern the high rates of biodiversity in small lowland water bodies altered by high anthropogenic pressure and climate-related impacts, such as the Šijanec gravel pit [67,68]. Previous studies on the Drava River lowland did not consider the importance of small water bodies within the whole alluvial system [69,70]. Due to hydromorphological characteristics of the catchment, Šijanec receives a high nitrogen input from the Drava River aquifer via groundwater recharging [41]. The high concentration of nitrates in the Drava River groundwater system, with an average of 60.9 mg L^{-1} , was observed by Marković et al. [41]. Nitrogen compounds can easily percolate through the soil into the groundwater either from direct terrestrial runoff or with rainfall or irrigation water [71]. A higher nitrogen concentration was noted during the colder seasons as a consequence of the recorded decrease in the phytoplankton biomass

and abundance, as well as the rise of the groundwater level due to an increase in precipitation [72,73], whereas nitrogen concentrations in the groundwater dropped during the warmer periods following the decrease of precipitation, as confirmed by the PCA analysis. Since nitrogen fertilizers are widely used in agriculture to increase crop production, the cropping practices and soil texture have been found to influence the extent of nitrate leaching [74].

The nutrient-based indication of eutrophic conditions in the gravel pit was further supported by high values of phytoplankton biomass and bacterial density throughout the investigated period, especially during the summer months, when the lowest NO_3^- concentration (June) and the highest concentrations of NH_4^+ and NO_2^- (July) were detected. This occurrence of elevated nitrogen is presumably occurring as an effect of the cropping season, e.g., fertilizer application through intense irrigation [75]. This is particularly true for nitrates, which are normally assumed not to be absorbed by soil particles and are therefore easily leached, in which case the nitrate distribution should follow the wetting front [76,77]. As found by Paredes et al. [78], high intra- and interannual hydrological fluctuations influenced nitrate occurrence in freshwater streams and ponds, with the main source of nitrate linked to agricultural practices and the use of both organic and synthetic fertilizers. Since it can be rapidly oxygenized, the concentration of NO_2^- is usually deficient [79], as was exhibited in this study. Most of the nitrogen uptake in shallow eutrophic systems is the form of nitrate, which has a positive effect on the growth of phytoplankton biomass [80,81]. A sample from June had the lowest concentrations of NO_3^- , TN, TIC, and $\log p\text{CO}_2$, but the highest temperature and Si values. These conditions were characterized by the dominance of cyanobacteria *Limnotrix redekei* and centric diatom *Aulacoseira muzzanensis*. *Limnotrix redekei*, a species characteristic of eutrophic shallow water bodies used for recreation and fishing, often shows domination in spring and summer periods with co-occurrence of centric diatoms [82]. This species is known for its ability to adapt to low-light, cold conditions and capability to overwinter in considerable densities under the long-term ice- and snow-cover [83–86]. *Aulacoseira muzzanensis*, a species adapted to live in turbid and nutrient-rich waters [87], was described in a hyper-eutrophic lake (Lago di Muzzano) located in the Tessin region of Switzerland [88], which suffers from periodic *Microcystis* algal blooms [89–92]. During lower light conditions, both taxa can occur concomitantly with the *Microcystis* species in quantities capable of eliminating other phytoplankton taxa [93]. A sample from July in the grouped composed of summer and autumn samples was characterized by maximum concentrations of nitrites and ammonium. This suggested enhanced growth conditions for specific algal groups under a higher NH_4^+ supply, which was also evident by a recorded high concentration of the chlorophyll *a*. Certain phytoplankton taxa, such as cyanobacteria and chlorophytes, prefer a high supply of energetically favorable NH_4^+ [94], as was also noted in our investigation. These conditions can also inhibit NO_3^- uptake for other taxa, such as large diatoms [94–96]. The most abundant chlorophyte was *Scenedesmus quadricauda*, a small coenobium-forming and ammonium-tolerant species [97–99] with higher uptake abilities for ammonium under nitrogen limitation than species of the genus *Microcystis* and with competitive superiority in the large-pulse, low-frequency nutrient recharging [100], as was present in our study area. With regard to size, small algae can be more competitive than larger species, because they have high surface area to volume ratios, resulting in greater specific uptake and growth under low nutrient concentrations, when even slight NH_4^+ additions can be enough to promote the growth of small algae [101]. Secondly, the most dominant species during the summer period was *Microcystis* spp., with the culmination of dominance (surface bloom) in August, which was connected with the maximum of phytoplankton biomass and number of cells per liter. *Microcystis* is a non- N_2 -fixing cyanobacteria, which dominates in highly eutrophicated, stratified ponds, rivers, or lakes receiving elevated N loadings, since its growth is dependent on nitrogen supplies [6]. A strong bloom of *Microcystis* spp. was associated with the warmer period, low nitrogen concentrations, and the subsequent water level drawdown [102]. Cyanobacteria have the ability to adapt to different environments

by adjusting their light harvesting and carbon fixation mechanisms. Adversely, a high rate of photosynthesis induced by the *Microcystis* bloom can considerably reduce dissolved CO₂ concentrations and drive up the pH value [103]. Furthermore, *Microcystis* favors more alkaline conditions as a competitive advantage over other phytoplankton groups [104,105]. Along with the *Microcystis* bloom, the molecular approach detected the cyanobacterium of the genus *Cyanobium*, which was dominant in August. *Cyanobium* is a picocyanobacterial genus with a presumably significant role in the functioning of aquatic ecosystems, but rather hard to detect microscopically due to its size and taxonomical obscurity. Both *Microcystis* and *Cyanobium* genera are less demanding on nutrients and generally demonstrate summer peaks when the concentrations of nitrogen compounds are usually lower [106]. As detected by the molecular approach, the phylum Planctomycetota was subdominant in the bacterial community in June. Members of the phylum Planctomycetota have been found in a variety of environments, including freshwater [107], and are known for their role in the anaerobic oxidation of ammonium (anammox), as part of the biogeochemical nitrogen cycle [108–112]. In oxygen-limited systems, such as biofilm aggregates, the planctomycete anammox bacteria live closely associated with aerobic ammonium oxidizers. The aerobic ammonium-oxidizing bacteria consume oxygen at the outside of the biofilm, thus keeping the inside anoxic for the anammox bacteria. Together, they create conditions in which they can convert ammonium directly into dinitrogen gas. Anammox bacteria can contribute significantly to the loss of fixed nitrogen in both natural and anthropogenic-influenced ecosystems [110,112,113]. The members of the phylum Bacteroidota recorded in July are typical for freshwater environments [114]. Their dominance correlated with OTUs taxonomically assigned in eukaryotic biflagellate cryptophytes from *Cryptomonas* genera, and with chlorophyte *Scenedesmus quadricauda*, as recorded by the morphological approach. The increase in their abundance correlated with higher algal concentrations, presumably due to their ability to establish a mutualistic relationship on the algal cell surface [115]. High densities of the *Cryptomonas* genus can occur following the period of nutrient enrichment [6]. During the colder period, the composition of the phytoplankton switched from cyanobacteria to a diatom-dominated community characterized by the genus *Ulnaria*, whose winter blooms require both biogenic silica for the formation of their outer cell wall structures (frustules) and lower basic pH conditions, as not to corrode them [116] and decrease the growth rate [117]. This resulted in a threefold drop in the SiO₂ concentration which was presumably consumed in the building of their frustules [118,119]. Diatoms are characterized as effective nitrate utilizers with high preferences to NO₃[−] uptake [120]. Also subdominant in the colder period, together with diatoms, were dinoflagellate species, which were reported to have significant NO₃[−] uptake rates [121]. A dense bloom of colonial chrysophyte *Dinobryon* spp. characterized the phytoplankton community in February and March. As adaptations to the lower temperature, the winter blooms of *Dinobryon* could indicate enhanced nutrient loading [6], but also the ability to obtain nutrients from bacteria by mixotrophy [122,123]. Members of Proteobacteria, as the most dominant bacterial phylum in the samples from November and December, are ubiquitous in freshwater environments, specifically in eutrophic conditions with high phytoplankton numbers [114,124]. Actinobacteriota were present throughout the investigated period, with increased abundance in October and January during the low abundance of cyanobacteria. This is plausibly correlated with the sensitivity of Actinobacteriota to conditions prevailing during the cyanobacterial blooms, such as high organic matter, inorganic nutrient availability, and high temperatures, under which the highly streamlined actinobacterial cells cannot compete [125]. Actinobacteriota can thrive under oligotrophic conditions due to their small size, high surface area-to-volume ratio, and enhanced capacity for efficient nutrient acquisition through high-affinity, broad-specific uptake systems [126]. Another important role of Actinobacteriota in freshwater habitats is connected to the proton-pumping rhodopsins (actinorhodopsins), thus revealing a photoheterotrophic lifestyle [127]. All these traits suggest that Actinobacteriota might serve as sentinels of impending ecological damage and have the potential to become standards of ecological freshwater quality [125].

Some of the OTUs were taxonomically assigned to species usually hard to detect under the microscope. These species included colonial chrysophyte *Uroglenopsis americana* (G.N.Calkins) Lemmermann, thecate dinoflagellate *Asulcocephalium miricentonis* Kazuya Takahashi, Moestrup & M. Iwataki and small green algae *Actinochloris sphaerica* Korschikov, *Meyerella planktonica* Fawley & K. P. Fawley, *Wislouchiella planktonica* Skvortzov and *Chloromonas subdivisa* (Pascher & Jahoda) Gerloff & Ettl. They were all detected in the winter samples, except for *Asulcocephalium miricentonis* and *Wislouchiella planktonica*, which were detected in June. Besides type locality, no further ecological data were available on *Asulcocephalium miricentonis*, a species described in a temperate freshwater artificial pond in northeastern Japan [128]. Therefore, this record presents a contribution to the ecological conditions in which the species likely occurs. *Wislouchiella planktonica* is associated with man-made reservoirs and lentic freshwater habitats with eutrophic conditions [129,130], which is in line with our findings. *Uroglenopsis americana* was detected in February together with *Dinobryon* spp., due to its ability to compete for nutrients during the colder period, unlike algal species in eutrophic conditions [131]. The picoplanktonic species *Meyerella planktonica* is a major component of aquatic systems and a significant primary producer regularly occurring during winter [132,133]. Some of the species from the *Chloromonas* genera were found in snow samples [134], as was the case with the species *Chloromonas subdivisa* detected during snowy winter conditions in Šijanec. *Actinochloris sphaerica* is a cosmopolitan species mostly recorded in soil cultures and puddles [135]. Since very scarce information is available on all these species, the presented results also contribute to elucidating their ecological preferences.

Both approaches showed variations in diversity richness. Based on the morphological approach, the maximum value of alpha diversity was recorded in June, presumably due to the favorable conditions for algal growth. The minimum value of alpha diversity was detected in February, due to the lower number of algal species, whereas by using the molecular approach, higher values of alpha diversity were detected in the colder period, which can be associated with two possible causes: (1) when cell abundances of specific taxa in the water sample drop below a specific threshold, they can still be detectable with the molecular approach, but may not be found by microscopy; and (2) the resting stages of some algal species cannot be identified and assigned correctly by microscopy, but might be more easily recorded by the molecular approach [136]. Moreover, the lowest value of alpha diversity detected in August with the molecular approach could be correlated with the cyanobacterial bloom. Some cyanobacteria are known to produce toxins and cyclic peptides which can inhibit regulatory enzymes in eukaryotic cells, thus causing PCR inhibition [137,138]. Similar variations were detected in bacterial alpha diversity, with a maximum in July and low values throughout August, September, and October. This finding also corresponds to cyanobacterial bloom, which can inhibit the stabilization of microbial diversity [139]. Surprisingly, the morphological approach, as a basic descriptive method, succeeded in recognizing a higher microalgal diversity in Šijanec than the molecular approach, which is commonly considered a more powerful detector tool [140]. Events such as cyanobacterial blooms or discrepancies in the various DNA extraction methods can also have a discernible impact on the certainty of the community analysis via the molecular approach. Eukaryotic algae have a large range of cell wall structures, thus imposing challenges to the unbiased, uniform, and universal extraction of nucleic acids from such communities [138]. In spite of this, the molecular approach proved far more effective in discerning small-sized eukaryotic algae and cyanobacterial taxa, which are generally hard to detect with microscopy due to the scarcity of taxonomic knowledge and limitations of resolving power. Molecular methods showed that they can be successfully used to complement the morphological approach for assessing the microbial community's structure [138,141], especially in these kinds of eutrophic environments.

5. Conclusions

Despite the size, small water bodies like the Šijanec gravel pit play a key role as buffer zones within alluvial areas of large rivers. Due to the hydromorphological characteristics of the catchment, Šijanec receives a high nitrate input directly from the groundwater recharging. Nitrogen compounds likely control the phytoplankton biomass, thereby influencing the complete microbial community's structure. The integration of morphological and molecular approaches facilitates the comprehensive assessment of the microbial community's structure. Interdisciplinary approaches can be successfully used to elucidate the ecological preferences of microbial species and the prediction and prevention of algal blooms. The study emphasizes the importance of small water bodies in maintaining the state of water ecosystems and stresses the need for their enlistment in biomonitoring actions.

Supplementary Materials: The following are available online at <https://www.mdpi.com/2073-4441/13/2/115/s1>. Document S1: includes the list of commands with related parameters used in the OBITools package.

Author Contributions: Formal analysis, investigation, data curation, writing—Original draft preparation, visualization, A.K.; chemical analysis, investigation, writing—Review and editing, T.M.; investigation, validation, writing—Review and editing, P.Ž.; data curation, writing—Review and editing, K.K.; description of the study area, investigation, writing—Review and editing, I.K.; methodology, investigation, writing—Review and editing, S.O.; software, writing—Review and editing, E.K.; validation, writing—Review and editing, V.F.; conceptualization, investigation, supervision, validation, writing—Review and editing M.G.U. All authors have read and agreed to the published version of the manuscript.

Funding: This study was supported by the Croatian Scientific Foundation (HRZZ), grant number HRZZ-IP-2016-06-5356, and by the COST DNAqua-Net grant (CA15219—"eDNA metabarcoding in providing assessment of microbial eukaryotic biodiversity in small standing-water ecosystem"). SO and KK were partially supported by the project STIM – REI, Contract Number: KK.01.1.1.01.0003, funded by the European Union through the European Regional Development Fund—the Operational Programme Competitiveness and Cohesion 2014–2020 (KK.01.1.1.01).

Institutional Review Board Statement: Not applicable.

Informed Consent Statement: Not applicable.

Data Availability Statement: The data presented in this study are available in: Kulaš, A.; Marković, T.; Žutinić, P.; Kajan, K.; Karlović, I.; Orlić, S.; Keskin, E.; Filipović, V.; Gligora Udovič, M. Succession of Microbial Community in a Small Water Body within the Alluvial Aquifer of a Large River Water *Water* **2021**, *13*, 115. <https://doi.org/10.3390/w13020115>.

Acknowledgments: We thank the evolutionary Genetics Laboratory (eGL) research team for their support and help in bioinformatics analysis.

Conflicts of Interest: The authors declare no conflict of interest.

References

1. Thingstad, T.; Sakshaug, E. Control of phytoplankton growth in nutrient recycling ecosystems. Theory and terminology. *Mar. Ecol. Prog. Ser.* **1990**, *63*, 261–272. [[CrossRef](#)]
2. Chan, J.L.; Mantzoros, C.S. Role of leptin in energy-deprivation states: Normal human physiology and clinical implications for hypothalamic amenorrhoea and anorexia nervosa. *Lancet* **2005**, *366*, 74–85. [[CrossRef](#)]
3. Green, P.; Vörösmarty, C.J.; Meybeck, M.; Galloway, J.N.; Peterson, B.J.; Boyer, E.W. Pre-industrial and contemporary fluxes of nitrogen through rivers: A global assessment based on typology. *Biogeochemistry* **2004**, *68*, 71–105. [[CrossRef](#)]
4. Li, Z.G.; Lin, B.-L.; Sagisaka, M.; Yang, P.; Wu, W. Global-scale modelling of potential changes in terrestrial nitrogen cycle from a growing nitrogen deposition. *Proc. Environ. Sci.* **2012**, *13*, 1057–1068. [[CrossRef](#)]
5. Galloway, J.N.; Cowling, E.B.; Seitzinger, S.; Socolow, R.H. Reactive nitrogen: Too much of a good thing? *Ambio* **2002**, *31*, 60–63. [[CrossRef](#)]
6. Paerl, H.W.; Fulton, R.S.; Moisaner, P.H.; Dyble, J. Harmful freshwater algal blooms, with an emphasis on Cyanobacteria. *Sci. World J.* **2001**, *1*, 76–113. [[CrossRef](#)]
7. Erisman, J.W.; Galloway, J.; Seitzinger, S.; Bleeker, A.; Butterbach-Bahl, K. Reactive nitrogen in the environment and its effect on climate change. *Curr. Opin. Environ. Sustain.* **2011**, *3*, 281–290. [[CrossRef](#)]

8. Dupas, R.; Delmas, M.; Dorioz, J.-M.; Garnier, J.; Moatar, F.; Gascuel-Oudou, C. Assessing the impact of agricultural pressures on N and P loads and eutrophication risk. *Ecol. Indic.* **2015**, *48*, 396–407. [[CrossRef](#)]
9. Erisman, J.W.; Galloway, J.N.; Seitzinger, S.; Bleeker, A.; Dise, N.B.; Petrescu, A.M.R.; Leach, A.M.; de Vries, W. Consequences of human modification of the global nitrogen cycle. *Philos. Trans. R. Soc. B Biol. Sci.* **2013**, *368*, 20130116. [[CrossRef](#)]
10. Mekonnen, M.M.; Hoekstra, A.Y. Global gray water footprint and water pollution levels related to anthropogenic nitrogen loads to fresh water. *Environ. Sci. Technol.* **2015**, *49*, 12860–12868. [[CrossRef](#)]
11. le Doux, E.; Gomez, E.; Monget, J.; Viavattene, C.; Viennot, P.; Ducharne, A.; Benoit, M.; Mignolet, C.; Schott, C.; Mary, B. Agriculture and groundwater nitrate contamination in the Seine basin. The STICS–MODCOU modelling chain. *Sci. Total Environ.* **2007**, *375*, 33–47. [[CrossRef](#)] [[PubMed](#)]
12. Mengel, K.; Hütsch, B.; Kane, Y. Nitrogen fertilizer application rates on cereal crops according to available mineral and organic soil nitrogen. *Eur. J. Agron.* **2006**, *24*, 343–348. [[CrossRef](#)]
13. Sete, P.B.; Comin, J.J.; Ciotta, M.N.; Salume, J.A.; Thewes, F.; Brackmann, A.; Toselli, M.; Nava, G.; Rozane, D.-E.; Loss, A.; et al. Nitrogen fertilization affects yield and fruit quality in pear. *Sci. Hortic.* **2019**, *258*, 108782. [[CrossRef](#)]
14. Jégo, G.; Sánchez-Pérez, J.M.; Justes, E. Predicting soil water and mineral nitrogen contents with the STICS model for estimating nitrate leaching under agricultural fields. *Agric. Water Manag.* **2012**, *107*, 54–65. [[CrossRef](#)]
15. Bernard-Jannin, L.; Sun, X.; Teissier, S.; Sauvage, S.; Sánchez-Pérez, J.M. Spatio-temporal analysis of factors controlling nitrate dynamics and potential denitrification hot spots and hot moments in groundwater of an alluvial floodplain. *Ecol. Eng.* **2017**, *103*, 372–384. [[CrossRef](#)]
16. Singer, G.; Besemer, K.; Schmitt-Kopplin, P.; Hödl, I.; Battin, T.J. Physical heterogeneity increases biofilm resource use and its molecular diversity in stream mesocosms. *PLoS ONE* **2010**, *5*, e9988. [[CrossRef](#)]
17. Cardinale, B.J.; Duffy, J.E.; Gonzalez, A.; Hooper, D.U.; Perrings, C.; Venail, P.; Narwani, A.; Mace, G.M.; Tilman, D.; Wardle, D.A.; et al. Biodiversity loss and its impact on humanity. *Nat. Cell Biol.* **2012**, *486*, 59–67. [[CrossRef](#)]
18. Besemer, K.; Singer, G.; Quince, C.; Bertuzzo, E.; Sloan, W.; Battin, T.J. Headwaters are critical reservoirs of microbial diversity for fluvial networks. *Proc. R. Soc. B* **2013**, *280*, 20131760. [[CrossRef](#)]
19. Widder, S.; Besemer, K.; Singer, G.A.; Ceola, S.; Bertuzzo, E.; Quince, C.; Sloan, W.T.; Rinaldo, A.; Battin, T.J. Fluvial network organization imprints on microbial co-occurrence networks. *Proc. Natl. Acad. Sci. USA* **2014**, *111*, 12799–12804. [[CrossRef](#)]
20. Peterson, B.J.; Wollheim, W.M.; Mulholland, P.J.; Webster, J.R.; Meyer, J.L.; Tank, J.L.; Martí, E.; Bowden, W.B.; Valett, H.M.; Hershey, A.E.; et al. Control of nitrogen export from watersheds by headwater streams. *Science* **2001**, *292*, 86–90. [[CrossRef](#)]
21. Paerl, H.W. Mitigating harmful cyanobacterial blooms in a human- and climatically impacted world. *Life* **2014**, *4*, 988–1012. [[CrossRef](#)]
22. Pal, R.; Choudhury, A.K. *An Introduction to Phytoplanktons: Diversity and Ecology*; Springer Science and Business Media LLC: Berlin/Heidelberg, Germany, 2014; pp. 25–52.
23. Herrero, A.; Muro-Pastor, A.M.; Flores, E. Nitrogen control in Cyanobacteria. *J. Bacteriol.* **2001**, *183*, 411–425. [[CrossRef](#)] [[PubMed](#)]
24. Stal, L. Cyanobacteria: Diversity and versatility. In *Algae and Cyanobacteria in Extreme Environments: Cellular Origin, Life in Extreme Habitats and Astrobiology*; Sedbach, J., Ed.; Springer: Dordrecht, The Netherlands, 2007; Volume 11, pp. 659–680.
25. Sellner, K.G. Physiology, ecology, and toxic properties of marine cyanobacteria blooms. *Limnol. Oceanogr.* **1997**, *42*, 1089–1104. [[CrossRef](#)]
26. Hemida, M.; Ohyam, T. Nitrogen fixing Cyanobacteria: Future prospect. *Nitrogen Fixat.* **2014**, 23–48. [[CrossRef](#)]
27. Bakker, E.S.; Hilt, S. Impact of water-level fluctuations on cyanobacterial blooms: Options for management. *Aquat. Ecol.* **2016**, *50*, 485–498. [[CrossRef](#)]
28. Hamilton, L.C. Public awareness of the scientific consensus on climate. *SAGE Open* **2016**, *6*. [[CrossRef](#)]
29. van Gremberghe, I.; Leliaert, F.; Mergeay, J.; Vanormelingen, P.; van der Gucht, K.; Debeer, A.-E.; Lacerot, G.; de Meester, L.; Vyverman, W. Lack of phylogeographic structure in the freshwater Cyanobacterium *Microcystis aeruginosa* suggests global dispersal. *PLoS ONE* **2011**, *6*, e19561. [[CrossRef](#)]
30. Gijzen, H.J.; Mulder, A. The nitrogen cycle out of balance. *Water* **2001**, *21*, 38–40.
31. Moss, B.; Barker, T.; Stephen, D.; Williams, A.E.; Balayla, D.J.; Beklioglu, M.; de Carvalho, L.P.S. Consequences of reduced nutrient loading on a lake system in a lowland catchment: Deviations from the norm? *Freshw. Biol.* **2005**, *50*, 1687–1705. [[CrossRef](#)]
32. Rosset, V.; Angélibert, S.; Arthaud, F.; Bornette, G.; Robin, J.; Wezel, A.; Vallod, D.; Oertli, B. Is eutrophication really a major impairment for small waterbody biodiversity? *J. Appl. Ecol.* **2014**, *51*, 415–425. [[CrossRef](#)]
33. Menetrey, N.; Sager, L.; Oertli, B.; Lachavanne, J.-B. Looking for metrics to assess the trophic state of ponds. Macroinvertebrates and amphibians. *Aquat. Conserv. Mar. Freshw. Ecosyst.* **2005**, *15*, 653–664. [[CrossRef](#)]
34. Søndergaard, M.; Jeppesen, E.; Jensen, J.P.; Amsinck, S.L. Water Framework Directive: Ecological classification of Danish lakes. *J. Appl. Ecol.* **2005**, *42*, 616–629. [[CrossRef](#)]
35. Williams, P.; Whitfield, M.; Biggs, J.; Bray, S.; Fox, G.; Nicolet, P.; Sear, D. Comparative biodiversity of rivers, streams, ditches and ponds in an agricultural landscape in Southern England. *Biol. Conserv.* **2004**, *115*, 329–341. [[CrossRef](#)]
36. Gvozdić, V.; Brana, J.; Puntarić, D.; Vidosavljević, D.; Roland, D. Changes in the Lower Drava River water quality parameters over 24 years. *Arch. Ind. Hyg. Toxicol.* **2011**, *62*, 325–333. [[CrossRef](#)]
37. Villanueva, J.; Rosell, A.; Grimalt, J.O.; Navarro, A.; Rosell-Melé, A. Chemical characterization of polycyclic aromatic hydrocarbon mixtures in uncontrolled hazardous waste dumps. *Chemosphere* **1991**, *22*, 317–326. [[CrossRef](#)]

38. Navarro, A.; Carbonell, M. Assessment of groundwater contamination caused by uncontrolled dumping in old gravel quarries in the Besòs aquifers (Barcelona, Spain). *Environ. Geochem. Health* **2007**, *30*, 273–289. [[CrossRef](#)]
39. Preziosi, E.; Frollini, E.; Zoppini, A.; Ghergo, S.; Melita, M.; Parrone, D.; Rossi, D.; Amalfitano, S. Disentangling natural and anthropogenic impacts on groundwater by hydrogeochemical, isotopic and microbiological data: Hints from a municipal solid waste landfill. *Waste Manag.* **2019**, *84*, 245–255. [[CrossRef](#)]
40. Ondrasek, G.; Begić, H.B.; Zovko, M.; Filipović, L.; Meriño-Gergichevich, C.; Savić, R.; Rengel, Z. Biogeochemistry of soil organic matter in agroecosystems & environmental implications. *Sci. Total Environ.* **2019**, *658*, 1559–1573. [[CrossRef](#)]
41. Marković, T.; Karlović, I.; Tadić, M.P.; Larva, O. Application of stable water isotopes to improve conceptual model of alluvial aquifer in the Varaždin area. *Water* **2020**, *12*, 379. [[CrossRef](#)]
42. Mandel, S.; Shiftan, Z.L. *Groundwater Resources: Investigation and Development*, 1st ed.; Academic Press: New York, NY, USA, 1980; pp. 180–200.
43. Domenico, P.A.; Schwartz, F.W. *Physical and Chemical Hydrogeology*, 2nd ed.; John Wiley and Sons: New York, NY, USA, 1990.
44. Parkhurst, D.L.; Appelo, C. User's guide to PHREEQC (Version 2): A computer program for speciation, batch-reaction, one-dimensional transport, and inverse geochemical calculations. *Water Res. Investig. Rep.* **1999**, *99*, 4259.
45. ISO/TC 147 Water Quality. Available online: <https://www.iso.org/committee/52834/x/catalogue/> (accessed on 16 April 2018).
46. Utermöhl, H. Zur vervollkommnung der quantitativen phytoplankton-methodik. Mitteilungen Internationale Vereinigung für Theoretische und Angewandte. *Limnologie* **1958**, *9*, 1–38.
47. Stock, A.; Jürgens, K.; Bunge, J.; Stoeck, T. Protistan diversity in suboxic and anoxic waters of the Gotland Deep (Baltic Sea) as revealed by 18S rRNA clone libraries. *Aquat. Microb. Ecol.* **2009**, *55*, 267–284. [[CrossRef](#)]
48. Stoeck, T.; Bass, D.; Nebel, M.; Christen, R.; Jones, M.D.M.; Breiner, H.-W.; Richards, T.A. Multiple marker parallel tag environmental DNA sequencing reveals a highly complex eukaryotic community in marine anoxic water. *Mol. Ecol.* **2010**, *19*, 21–31. [[CrossRef](#)] [[PubMed](#)]
49. Amaral-Zettler, L.; McCliment, E.A.; Ducklow, H.W.; Huse, S.M. A method for studying protistan diversity using massively parallel sequencing of V9 hypervariable regions of small-subunit ribosomal RNA genes. *PLoS ONE* **2009**, *4*, e6372. [[CrossRef](#)]
50. Herlemann, D.P.R.; Labrenz, M.; Jürgens, K.; Bertilsson, S.; Waniek, J.J.; Andersson, A.F. Transitions in bacterial communities along the 2000 km salinity gradient of the Baltic Sea. *ISME J.* **2011**, *5*, 1571–1579. [[CrossRef](#)]
51. de Barba, M.; Miquel, C.; Boyer, F.; Mercier, C.; Rioux, D.; Coissac, E.; Taberlet, P. DNA metabarcoding multiplexing and validation of data accuracy for diet assessment: Application to omnivorous diet. *Mol. Ecol. Resour.* **2013**, *14*, 306–323. [[CrossRef](#)] [[PubMed](#)]
52. Bellemain, E.; Carlsen, T.; Brochmann, C.; Coissac, E.; Taberlet, P.; Kauserud, H. ITS as an environmental DNA barcode for fungi: An in silico approach reveals potential PCR biases. *BMC Microbiol.* **2010**, *10*, 189. [[CrossRef](#)]
53. Ficetola, G.F.; Coissac, E.; Zundel, S.; Riaz, T.; Shehzad, W.; Bessière, J.; Taberlet, P.; Pompanon, F. An *in-silico* approach for the evaluation of DNA barcodes. *BMC Genom.* **2010**, *11*, 434. [[CrossRef](#)]
54. BBMap. Available online: <https://sourceforge.net/projects/bbmap/> (accessed on 19 February 2019).
55. Caporaso, J.G.; Kuczynski, J.; Stombaugh, J.; Bittinger, K.; Bushman, F.D.; Costello, E.K.; Fierer, N.; Peña, A.G.; Goodrich, J.K.; Gordon, J.I.; et al. QIIME allows analysis of high-throughput community sequencing data. *Nat. Methods* **2010**, *7*, 335–336. [[CrossRef](#)]
56. Edgar, R.C.; Haas, B.J.; Clemente, J.C.; Quince, C.; Knight, R. UCHIME improves sensitivity and speed of chimera detection. *Bioinformatics* **2011**, *27*, 2194–2200. [[CrossRef](#)]
57. Mahé, F.; Rognes, T.; Quince, C.; de Vargas, C.; Dunthorn, M. Swarm v2: Highly scalable and high-resolution amplicon clustering. *PeerJ* **2015**, *3*, e1420. [[CrossRef](#)] [[PubMed](#)]
58. Altschul, S.F.; Gish, W.; Miller, W.; Myers, E.W.; Lipman, D.J. Basic local alignment search tool. *J. Mol. Biol.* **1990**, *215*, 403–410. [[CrossRef](#)]
59. R Core Team. *R: A Language and Environment for Statistical Computing*; R Core Team: Vienna, Austria, 2020.
60. Tapolczai, K.; Vasselon, V.; Lefrançois, E.; Stenger-Kovács, C.; Padisák, J.; Rimet, F. The impact of OTU sequence similarity threshold on diatom-based bioassessment: A case study of the rivers of Mayotte (France, Indian Ocean). *Ecol. Evol.* **2019**, *9*, 166–179. [[CrossRef](#)] [[PubMed](#)]
61. Anderson, M.J. Distance-based tests for homogeneity of multivariate dispersions. *Biometrics* **2005**, *62*, 245–253. [[CrossRef](#)] [[PubMed](#)]
62. Oksanen, J.; Blanchet, F.G.; Friendly, M.; Kindt, R.; Legendre, P.; McGlinn, D.; Minchin, P.R.; O'Hara, R.B.; Simpson, G.L.; Solymos, P.; et al. Vegan: Community Ecology Package. *R Packag. Vers.* **2015**, *2*, 1–2.
63. Bolpagni, R.; Poikane, S.; Laini, A.; Bagella, S.; Bartoli, M.; Cantonati, M. Ecological and conservation value of small standing-water ecosystems: A systematic review of current knowledge and future challenges. *Water* **2019**, *11*, 402. [[CrossRef](#)]
64. Céréghino, R.; Boix, D.; Cauchie, H.-M.; Martens, K.; Oertli, B. The ecological role of ponds in a changing world. *Hydrobiologia* **2014**, *723*, 1–6. [[CrossRef](#)]
65. Brönmark, C.; Hansson, L.-A. Environmental issues in lakes and ponds: Current state and perspectives. *Environ. Conserv.* **2002**, *29*, 290–307. [[CrossRef](#)]
66. Hering, D.; Haidekker, A.; Schmidt-Kloiber, A.; Barker, T.; Buisson, L.; Graf, W.; Grenouillet, G.; Lorenz, A.; Sandin, L.; Stendera, S. Monitoring the responses of freshwater ecosystems to climate change. *Clim. Chang. Impacts Freshw. Ecosyst.* **2010**, *84*–118. [[CrossRef](#)]

67. Boix, D.; Biggs, J.; Céréghino, R.; Hull, A.P.; Kalettka, T.; Oertli, B. Pond research and management in Europe: “Small is Beautiful”. *Hydrobiologia* **2012**, *689*, 1–9. [[CrossRef](#)]
68. Bagella, S.; Gascón, S.; Filigheddu, R.; Cogoni, A.; Boix, D. Mediterranean temporary ponds: New challenges from a neglected habitat. *Hydrobiologia* **2016**, *782*, 1–10. [[CrossRef](#)]
69. Stanković, I.; Vlahović, T.; Udovič, M.G.; Várbiro, G.; Borics, G. Phytoplankton functional and morpho-functional approach in large floodplain rivers. *Hydrobiologia* **2012**, *698*, 217–231. [[CrossRef](#)]
70. Kovács, A.D.; Tóth, G.; Lóczy, D. *Water Quality of the Lower Drava River*; Springer Science and Business Media LLC: Berlin/Heidelberg, Germany, 2018; pp. 231–245.
71. Gao, K.; Helbling, E.; Häder, D.; Hutchins, D. Responses of marine primary producers to interactions between ocean acidification, solar radiation, and warming. *Mar. Ecol. Prog. Ser.* **2012**, *470*, 167–189. [[CrossRef](#)]
72. van Verseveld, W.J.; McDonnell, J.J.; Lajtha, K. The role of hillslope hydrology in controlling nutrient loss. *J. Hydrol.* **2009**, *367*, 177–187. [[CrossRef](#)]
73. Jiang, R.; Woli, K.P.; Kuramochi, K.; Hayakawa, A.; Shimizu, M.; Hatano, R. Hydrological process controls on nitrogen export during storm events in an agricultural watershed. *Soil Sci. Plant Nutr.* **2010**, *56*, 72–85. [[CrossRef](#)]
74. Serio, F.; Miglietta, P.P.; Lamastra, L.; Ficocelli, S.; Intini, F.; de Leo, F.; de Donno, A. Groundwater nitrate contamination and agricultural land use: A grey water footprint perspective in Southern Apulia Region (Italy). *Sci. Total Environ.* **2018**, *645*, 1425–1431. [[CrossRef](#)] [[PubMed](#)]
75. Filipovic, V.; Kodešová, R.; Petosic, D. Experimental and mathematical modeling of water regime and nitrate dynamics on zero tension plate lysimeters in soil influenced by high groundwater table. *Nutr. Cycl. Agroecosyst.* **2012**, *95*, 23–42. [[CrossRef](#)]
76. Filipović, V.; Romić, D.; Romić, M.; Borošić, J.; Filipović, L.; Mallmann, F.J.K.; Robinson, D.A. Plastic mulch and nitrogen fertigation in growing vegetables modify soil temperature, water and nitrate dynamics: Experimental results and a modeling study. *Agric. Water Manag.* **2016**, *176*, 100–110. [[CrossRef](#)]
77. Hardie, M.; Ridges, J.; Swarts, N.; Close, D.C. Drip irrigation wetting patterns and nitrate distribution: Comparison between electrical resistivity (ERI), dye tracer, and 2D soil–water modelling approaches. *Irrig. Sci.* **2018**, *36*, 97–110. [[CrossRef](#)]
78. Paredes, I.; Otero, N.; Soler, A.; Green, A.J.; Soto, D.X. Agricultural and urban delivered nitrate pollution input to Mediterranean temporary freshwaters. *Agric. Ecosyst. Environ.* **2020**, *294*, 106859. [[CrossRef](#)]
79. Wetzel, R.G. *Limnology: Lake and River Ecosystems*, 3rd ed.; Academic Press: San Diego, CA, USA, 2001; pp. 239–288.
80. Kanda, F.; Yagi, E.; Fukuda, M.; Nakajima, K.; Ohta, T.; Nakata, O. Elucidation of chemical compounds responsible for foot malodour. *Br. J. Dermatol.* **1990**, *122*, 771–776. [[CrossRef](#)]
81. Strom, S. Novel interactions between phytoplankton and microzooplankton: Their influence on the coupling between growth and grazing rates in the sea. *Hydrobiologia* **2002**, *480*, 41–54. [[CrossRef](#)]
82. Budzyńska, A.; Goldyn, R.; Zagajewski, P.; Dondajewska, R.; Kowalczywska-Madura, K. The dynamics of a *Planktothrix agardhii* population in a shallow dimictic lake. *Oceanol. Hydrobiol. Stud.* **2009**, *38*, 1–6.
83. Meffert, M.F. Planktic unsheathed filaments (Cyanophyceae) with polar and central gas-vacuoles. II. Biology population dynamics and biotopes of *Limnothrix redekei* (Van Goor) Meffert. *Arch. Hydrobiol.* **1989**, *116*, 257–282.
84. Trifonova, I.S. *Ecology and Succession of Lake Phytoplankton*; Nauka Press: Leningrad, Russia, 1990.
85. Wiedner, C.; Nixdorf, B. Success of chrysophytes, cryptophytes and dinoflagellates over blue green (cyanobacteria) during an extreme winter (1995/96) in eutrophic shallow lakes. *Hydrobiologia* **1998**, *369*, 229–235. [[CrossRef](#)]
86. Romanov, R.E. *Limnothrix redekei* (Van Goor) Meffert (Cyanoprocarota) in the potamoplankton. *Int. J. Algae* **2007**, *9*, 105–116. [[CrossRef](#)]
87. Licursi, M.; Sierra, M.V.; Gómez, N. Diatom assemblages from a turbid coastal plain estuary: Río de la Plata (South America). *J. Mar. Syst.* **2006**, *62*, 35–45. [[CrossRef](#)]
88. Meister, F. Die Kieselalgen der Schweiz. In *Beiträge zur Kryptogamenflora der Schweiz*; Wyss, K.J., Ed.; K.J. Wyss: Bern, Switzerland, 1912; Volume 4, p. 254.
89. Bottinelli, M. Fioriture di Cianobatteri della specie *Microcystis wesenbergii* nel Lago di Muzzano. Ph.D. Thesis, Tesi Sperimentale di Laurea in Scienze Naturali, Università degli Studi di Pavia, Pavia, Italy, 1999; p. 172.
90. Bottinelli, M.; Tonolla, M.; Forlani, G.; Crivelli, C.; Sanangelantoni, A.M.; e Peduzzi, R. Fioriture di Cianobatteri della specie *Microcystis wesenbergii* nel Lago di Muzzano (Svizzera). *Boll. Della Soc. Tic. Di Sci. Nat.* **2000**, *88*, 53–61.
91. Isenburg, C.; Loizeau, J.L.; Tonolla, M.; Peduzzi, R. Aspetti limnologici e microbiologici del Laghetto di Muzzano (TI). *Boll. Soc. Tic. Sci. Nat.* **2000**, *88*, 41–51.
92. Pedrotta, T. Analisi qualitativa degli immissari e dell’emissario del Laghetto di Muzzano. Tesi di Laurea in AGRN. *Front. Ecol. Evolut.* **2009**, *3*, 70.
93. Reynolds, C. *Ecology of Phytoplankton*; Cambridge University Press: Cambridge, UK, 2006.
94. Glibert, P.M.; Wilkerson, F.P.; Dugdale, R.C.; Raven, J.A.; Dupont, C.L.; Leavitt, P.R.; Parker, A.E.; Burkholder, J.M.; Kana, T.M. Pluses and minuses of ammonium and nitrate uptake and assimilation by phytoplankton and implications for productivity and community composition, with emphasis on nitrogen-enriched conditions. *Limnol. Oceanogr.* **2016**, *61*, 165–197. [[CrossRef](#)]
95. Eppley, R.W.; Coatsworth, J.L.; Solórzano, L. Studies of nitrate reductase in marine phytoplankton. *Limnol. Oceanogr.* **1969**, *14*, 194–205. [[CrossRef](#)]

96. Sommer, U. Disturbance-diversity relationships in two lakes of similar nutrient chemistry but contrasting disturbance regimes. *Hydrobiologia* **1993**, *249*, 59–65. [[CrossRef](#)]
97. Miyazaki, T.; Honjo, Y.; Ichimura, S. Applicability of the stable isotope method using ¹³C and ¹⁵N simultaneously to the estimation of carbon and nitrogen assimilation in a eutrophic, freshwater lake, Lake Nakanuma, Japan. *Arch. Hydrobiol.* **1985**, *102*, 355–365.
98. Karya, N.; van der Steen, N.; Lens, P. Photo-oxygenation to support nitrification in an algal–bacterial consortium treating artificial wastewater. *Bioresour. Technol.* **2013**, *134*, 244–250. [[CrossRef](#)]
99. Hou, X.L.; Ma, D.L.; Yang, K.F.; Wang, R.; Rong, D.L.; Yin, X.T. The physiological responses of one algae species *Scenedesmus quadricauda* to ammonium and alanine. *IOP Conf. Ser. Earth Environ. Sci.* **2019**, *344*, 012167. [[CrossRef](#)]
100. Watanabe, T.; Miyazaki, T. Maximum ammonium uptake rates of *Scenedesmus quadricauda* (Chlorophyta) and *Microcystis novacekii* (Cyanobacteria) grown under nitrogen limitation and implications for competition. *J. Phycol.* **1996**, *32*, 243–249. [[CrossRef](#)]
101. Trommer, G.; Poxleitner, M.; Stibor, H. Responses of lake phytoplankton communities to changing inorganic nitrogen supply forms. *Aquat. Sci.* **2020**, *82*, 22. [[CrossRef](#)]
102. Barone, R.; Naselli-Flores, L. Distribution and seasonal dynamics of cryptomonads in Sicilian water bodies. *Hydrobiologia* **2003**, *502*, 325–329. [[CrossRef](#)]
103. Paerl, H.W. Mitigating toxic planktonic cyanobacterial blooms in aquatic ecosystems facing increasing anthropogenic and climatic pressures. *Toxins* **2018**, *10*, 76. [[CrossRef](#)]
104. Hutchinson, G.E. The paradox of the plankton. *Am. Nat.* **2002**, *95*, 137–145. [[CrossRef](#)]
105. Wilhelm, S.W.; Bullerjahn, G.S.; McKay, R.M.L. The complicated and confusing ecology of *Microcystis* blooms. *mBio* **2020**, *11*, 00529–20. [[CrossRef](#)] [[PubMed](#)]
106. Belykh, O.I.; Dmitrieva, O.A.; Gladkikh, A.S.; Sorokovikova, E.G. Identification of toxigenic Cyanobacteria of the genus *Microcystis* in the Curonian Lagoon (Baltic Sea). *Oceanology* **2013**, *53*, 71–79. [[CrossRef](#)]
107. Fuerst, J.A. Planctomycetes—new models for microbial cells and activities. *Microb. Res.* **2017**, 1–27. [[CrossRef](#)]
108. Strous, M.; Kuenen, J.G.; Jetten, M.S.M. Key physiology of anaerobic ammonium oxidation. *Appl. Environ. Microbiol.* **1999**, *65*, 3248–3250. [[CrossRef](#)] [[PubMed](#)]
109. Jetten, M.S.; Wagner, M.; Fuerst, J.; van Loosdrecht, M.; Kuenen, G.; Strous, M. Microbiology and application of the anaerobic ammonium oxidation (‘anammox’) process. *Curr. Opin. Biotechnol.* **2001**, *12*, 283–288. [[CrossRef](#)]
110. Jetten, M.S.; Sliemers, O.; Kuypers, M.M.M.; Dalsgaard, T.K.; van Niftrik, L.; Cirpus, I.; van de Pas-Schoonen, K.; Lavik, G.; Thamdrup, B.; le Paslier, D.; et al. Anaerobic ammonium oxidation by marine and freshwater planctomycete-like bacteria. *Appl. Microbiol. Biotechnol.* **2003**, *63*, 107–114. [[CrossRef](#)]
111. Schmid, M.; Schmitz-Esser, S.; Jetten, M.; Wagner, M. 16S–23S rDNA intergenic spacer and 23S rDNA of anaerobic ammonium-oxidizing bacteria: Implications for phylogeny and *in situ* detection. *Environ. Microbiol.* **2001**, *3*, 450–459. [[CrossRef](#)]
112. Kuypers, M.M.M.; Sliemers, A.O.; Lavik, G.; Schmid, M.; Jørgensen, B.B.; Kuenen, J.G.; Damsté, J.S.S.; Strous, M.; Jetten, M.S.M. Anaerobic ammonium oxidation by anammox bacteria in the Black Sea. *Nat. Cell Biol.* **2003**, *422*, 608–611. [[CrossRef](#)]
113. van de Graaf, A.A.; de Bruijn, P.; Robertson, L.A.; Jetten, M.S.M.; Kuenen, J.G. Metabolic pathway of anaerobic ammonium oxidation on the basis of ¹⁵N studies in a fluidized bed reactor. *Microbiology* **1997**, *143*, 2415–2421. [[CrossRef](#)]
114. Newton, P.N.; Amin, A.A.; E Bird, C.; Passmore, P.; Dukes, G.; Tomson, G.; Simons, B.; Bate, R.; Guerin, P.J.; White, N.J. The primacy of public health considerations in defining poor quality medicines. *PLoS Med.* **2011**, *8*, e1001139. [[CrossRef](#)] [[PubMed](#)]
115. Russo, D.A.; Couto, N.; Beckerman, A.P.; Pandhal, J. A metaproteomic analysis of the response of a freshwater microbial community under nutrient enrichment. *Front. Microbiol.* **2016**, *7*, 1172. [[CrossRef](#)] [[PubMed](#)]
116. Martin-Jezequel, V.; Hildebrand, M.; Brzezinski, M.A. Silicon metabolism in diatoms: Implications for growth. *J. Phycol.* **2000**, *36*, 821–840. [[CrossRef](#)]
117. Lundholm, N.; Moestrup, Ø.; Kotaki, Y.; Hoef-Emden, K.; Scholin, C.; Miller, P. Inter- and intraspecific variation of the *Pseudo-nitzschia delicatissima* complex (Bacillariophyceae) illustrated by rRNA probes, morphological data and phylogenetic analyses. *J. Phycol.* **2006**, *42*, 464–481. [[CrossRef](#)]
118. Nelson, D.M.; Dortch, Q. Silicic acid depletion in the plume of the Mississippi River and limitation of Si availability to diatoms in the northern Gulf of Mexico: Evidence from kinetic studies in spring and summer. *Mar. Ecol. Prog. Ser.* **1996**, *136*, 163–178. [[CrossRef](#)]
119. Gibson, C.E.; Wang, G.; Foy, R.H. Silica and diatom growth in Lough Neagh: The importance of internal recycling. *Freshw. Biol.* **2000**, *45*, 285–293. [[CrossRef](#)]
120. Glibert, P.M.; Wilkerson, F.P.; Dugdale, R.C.; Parker, A.E.; Alexander, J.A.; Blaser, S.; Murasko, S. Phytoplankton communities from San Francisco Bay Delta respond differently to oxidized and reduced nitrogen substrates—even under conditions that would otherwise suggest nitrogen sufficiency. *Front. Mar. Sci.* **2014**, *1*, 17. [[CrossRef](#)]
121. Dortch, Q. The interaction between ammonium and nitrate uptake in phytoplankton. *Mar. Ecol. Prog. Ser.* **1990**, *61*, 183–201. [[CrossRef](#)]
122. Kamjunke, N.; Henrichs, T.; Gaedke, U. Phosphorus gain by bacterivory promotes the mixotrophic flagellate *Dinobryon* spp. during re-oligotrophication. *J. Plankton Res.* **2006**, *29*, 39–46. [[CrossRef](#)]
123. Žutinić, P.; Gligora Udovič, M.; Kralj Borojević, K.; Plenković-Moraj, A.; Padisák, J. Morpho-functional classifications of phytoplankton assemblages of two deep karstic lakes. *Hydrobiologia* **2014**, *740*, 147–166. [[CrossRef](#)]

124. Eiler, A.; Bertilsson, S. Flavobacteria blooms in four eutrophic lakes: Linking population dynamics of freshwater bacterioplankton to resource availability. *Appl. Environ. Microbiol.* **2007**, *73*, 3511–3518. [[CrossRef](#)] [[PubMed](#)]
125. Ghai, R.; Mizuno, C.M.; Picazo, A.; Camacho, A.; Rodriguez-Valera, F. Key roles for freshwater Actinobacteria revealed by deep metagenomic sequencing. *Mol. Ecol.* **2014**, *23*, 6073–6090. [[CrossRef](#)] [[PubMed](#)]
126. Lauro, F.M.; McDougald, D.; Thomas, T.; Williams, T.J.; Egan, S.; Rice, S.; DeMaere, M.Z.; Ting, L.; Ertan, H.; Johnson, J.; et al. The genomic basis of trophic strategy in marine bacteria. *Proc. Natl. Acad. Sci. USA* **2009**, *106*, 15527–15533. [[CrossRef](#)] [[PubMed](#)]
127. Sharma, A.K.; Sommerfeld, K.; Bullerjahn, G.S.; Matteson, A.R.; Wilhelm, S.W.; Jezbera, J.; Brandt, U.; Doolittle, W.F.; Hahn, M.W. Actinorhodopsin genes discovered in diverse freshwater habitats and among cultivated freshwater Actinobacteria. *ISME J.* **2009**, *3*, 726–737. [[CrossRef](#)] [[PubMed](#)]
128. Takahashi, K.; Moestrup, Ø.; Jordan, R.W.; Iwataki, M. Two new freshwater Woloszynskioids *Asulcocephalium miricentonis* gen. et sp. nov. and *Leiocephalium pseudosanguineum* gen. et sp. nov. (Suessiaceae, Dinophyceae) lacking an apical furrow apparatus. *Protist* **2015**, *166*, 638–658. [[CrossRef](#)] [[PubMed](#)]
129. Reveal, J.L. *Wislouchiella planctonica* Skvortz. (Chlorophyta, Volvocales), a new algal record for Nevada. *Great Basin Nat.* **1969**, *29*, 3–4.
130. Broady, P.A.; Flint, E.A.; Nelson, W.A.; Cassie Cooper, V.; de Winton, M.D.; Novis, P.M. Phylum Chlorophyta and Charophyta: Green algae. In *New Zealand Inventory of Biodiversity, Kingdoms Bacteria, Protozoa, Chromista, Plantae, Fungi*; Gordon, D.P., Ed.; Canterbury University Press: Christchurch, New Zealand, 2012; Volume 3, pp. 347–381.
131. Felip, M.; Sattler, B.; Psenner, R.; Catalan, J. Highly active microbial communities in the ice and snow cover of high mountain lakes. *Appl. Environ. Microbiol.* **1995**, *61*, 2394. [[CrossRef](#)]
132. Callieri, C.; Stockner, J.G. Freshwater autotrophic picoplankton: A review. *J. Limnol.* **2002**, *61*, 1–14. [[CrossRef](#)]
133. Fawley, M.W.; Fawley, K.P.; Buchheim, M.A. Molecular diversity among communities of freshwater microchlorophytes. *Microb. Ecol.* **2004**, *48*, 489–499. [[CrossRef](#)]
134. Muramoto, K.; Nakada, T.; Shitara, T.; Hara, Y.; Nozaki, H. Re-examination of the snow algal species *Chloromonas mituae* (Fukushima) Muramoto et al., comb. nov. (Volvocales, Chlorophyceae) from Japan, based on molecular phylogeny and cultured material. *Eur. J. Phycol.* **2010**, *45*, 27–37. [[CrossRef](#)]
135. Mikhailyuk, T.; Glaser, K.; Tsarenko, P.; Demchenko, E.; Karsten, U. Composition of biological soil crusts from sand dunes of the Baltic Sea coast in the context of an integrative approach to the taxonomy of microalgae and cyanobacteria. *Eur. J. Phycol.* **2019**, *54*, 263–290. [[CrossRef](#)]
136. Medinger, R.; Nolte, V.; Pandey, R.V.; Jost, S.; Ottenwälder, B.; Schlötterer, C.; Boenigk, J. Diversity in a hidden world: Potential and limitation of next-generation sequencing for surveys of molecular diversity of eukaryotic microorganisms. *Mol. Ecol.* **2010**, *19*, 32–40. [[CrossRef](#)]
137. Mackintosh, C.; Beattie, K.A.; Klumpp, S.; Cohen, P.; Codd, G.A. Cyanobacterial microcystin-LR is a potent and specific inhibitor of protein phosphatases 1 and 2A from both mammals and higher plants. *FEBS Lett.* **1990**, *264*, 187–192. [[CrossRef](#)]
138. Eland, L.E.; Davenport, R.J.; Mota, C. Evaluation of DNA extraction methods for freshwater eukaryotic microalgae. *Water Res.* **2012**, *46*, 5355–5364. [[CrossRef](#)] [[PubMed](#)]
139. Rashidan, K.K.; Bird, D.F. Role of predatory bacteria in the termination of a cyanobacterial bloom. *Microb. Ecol.* **2001**, *41*, 97–105. [[CrossRef](#)] [[PubMed](#)]
140. Ghosh, S.; Love, N.G. Application of rbcL based molecular diversity analysis to algae in wastewater treatment plants. *Bioresour. Technol.* **2011**, *102*, 3619–3622. [[CrossRef](#)]
141. van Elsas, J.D.; Boersma, F.G.H. A review of molecular methods to study the microbiota of soil and the mycosphere. *Eur. J. Soil Biol.* **2011**, *47*, 77–87. [[CrossRef](#)]